

COMPETITION AND SUCCESSION OF KEY MARINE PHYTOPLANKTON
FUNCTIONAL GROUPS IN A VARIABLE ENVIRONMENT

by

Sasha Tozzi

A thesis submitted to the

Graduate School-New Brunswick

Rutgers, The State University of New Jersey

in partial fulfillment of the requirements

for the degree of

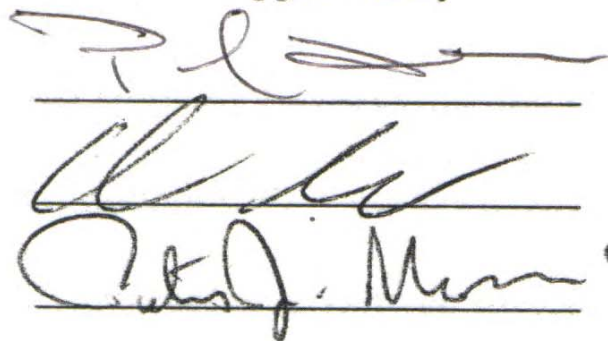
Master of Sciences

Graduate Program in Oceanography

written under the direction of

Paul G. Falkowski

and approved by

Three handwritten signatures are written on three horizontal lines. The top signature is in dark ink and appears to be 'P. Falkowski'. The middle signature is in dark ink and appears to be 'S. Tozzi'. The bottom signature is in dark ink and appears to be 'C. J. Morris'.

New Brunswick, New Jersey

October, 2001

ABSTRACT OF THE DISSERTATION

COMPETITION AND SUCCESSION OF KEY MARINE PHYTOPLANKTON FUNCTIONAL GROUPS IN A VARIABLE ENVIRONMENT

by Sasha Tozzi

Dissertation Director:

Paul G. Falkowski

The goal of this thesis is understand how the physiological ecology of phytoplankton impacts the competitive success between biogeochemically-significant phytoplankton taxa. More specifically, the effect of a variable nutrient regime on resource competition and successions between diatoms and coccolithophores was studied using a prognostic numerical model. Numerical simulations assessing the impact of nutrient vacuole present in diatoms but not in coccolithophorids were conducted and results were verified with laboratory experiments. The vacuoles advantage diatoms with pulses up to 24 hours or few divisions. Diatoms result then to prevail in a high turbulent mixing environment with high nutrient concentrations and coccolithophores in a more stable and depleted water column.

Table of contents

ABSTRACT OF THE DISSERTATION	ii
Table of contents	iii
List of illustration.....	vii
List of tables.....	ix
1 Introduction.....	1
1.2 Succession and resource competition: theory and related algal growth models..	5
1.2.1. Monod model	6
1.2.2. Droop model	9
1.3 Phytoplankton functional groups	11
1.4 Coccolithophores	13
1.4.1. Biology and physiology	15
1.4.2 Diversity and biogeography	17
1.5 Diatoms	20
1.5.1 Biology and physiology	21
1.5.2 Diversity and biogeography	22
2 Material and Methods	24
2.1. Growth rates and cell size	24
2.2. Chlorophyll a	25
2.3 Fast Repetition Rate (FRR) fluorescence	25
2.4 Emiliania huxleyi N cell quota	26
2.5 Nutrients.....	26
2.6 Emiliania huxleyi nitrate uptake	28

2.7	Competition experiment.....	28
2.8	Numerical simulation.....	28
3	Results.....	30
3.1	Emiliana huxleyi and Thalassiosira pseudonana growth rates and variable fluorescence	30
3.2	Emiliana huxleyi N and total C cell quotas	32
3.3	Emiliana huxleyi nitrate uptake	33
3.4	Competition experiment.....	33
3.5	Numerical simulation.....	36
3.5.1	Monod model.....	38
3.5.2	Mixed Droop-Monod model	51
4	Discussion	60
5	Prospect.....	62
	Appendix (Source code)	64
	Monod model	64
	Main code (Monod)	64
	Function M0.....	67
	Function M2.....	67
	Function Pulse1	68
	Mixed Droop-Monod model	69
	Main code (Droop).....	69
	Function D0	72
	Function D2	73

Bibliography	74
--------------------	----

List of illustration

Figure 1. Alternation between successional dynamics and discontinuous resetting. On the left water column thermocline variation during a year in relation to planktonic succession. On the right seasonal variation of water temperature, mixing, heat amount in water and energy. From (Margalef 1997)	3
Figure 2. The phytoplankton "mandala". Dominance and succession of different phytoplankton organism it is explained with a correlation between different combinations of environmental factors. From (Margalef 1997).....	3
Figure 3. Growth function for <i>Emiliania huxleyi</i> (red line) and <i>Thalassiosira pseudonana</i> (green line) according a Monod model. The two organisms are parameterized as described in (Table 4).	8
Figure 4. SEM photography of <i>Emiliania huxleyi</i> (http://www.soc.soton.ac.uk/SUDO/tt/eh/).....	13
Figure 5 Annual composite of classified coccolithophore blooms in SeaWiFS imagery dating from October 1997 to September 1999. The bloom class is white, the non-coccolithophore bloom class is blue, the land is black and the ice is gray	18
Figure 6. Evolution of the major eucaryotic phytoplankton taxa from Delwiche (1999).	19
Figure 7. Annual production of opaline silica in the world ocean ($\text{g Si}_2 \text{ m}^{-2} \text{ y}^{-1}$) (from Lisitzin, 1972). Key: 1= <100; 2= 100-250; 3=250-500; 4=>500. The cross-hatched area at 15°S and 180°W is from a printing error in early primary productivity maps and should be <100 (see Berger et al 1987, p.49).....	23
Figure 8. Growth rate and variable florescence for (a) <i>Thalassiosira pseudonana</i> ; (b) <i>Emiliania huxleyi</i>	31
Figure 9. Total C:N in <i>Emiliania huxleyi</i> determined by CHN.	32
Figure 10. Normalized cell density in the three treatments of the competition experiment. <i>Emiliania huxleyi</i> (red solid line) in the control flask, (broken red line) in the mix batch; <i>Thalassiosira pseudonana</i> (green solid line) in the control flask, (broken green line) in the mix batch.	34
Figure 11. Time course of nutrients during the competition experiment in the three treatments. Monospecific batch culture of <i>Emiliania huxleyi</i> (red solid line); monospecific batch culture of <i>Thalassiosira pseudonana</i> (green solid line); mixed culture (blue broken line) (a) nitrate; (b) silicate; (c) phosphate.	35
Figure 12. Power spectra of turbulence showing current data from ADCP from the Middle Atlantic Bight. Spectra were determined from 1048 hours long measurements with 50% overlaps. The first shows the spectra of the east and north components, plus the total spectrum, which is the sum of the spectra from the components, from 12.5 meters. (courtesy of Dr. C.N. Flagg)	37
Figure 13. (a) Cell density of <i>Emiliania huxleyi</i> (red solid line) and <i>Thalassiosira pseudonana</i> (green solid line); (b) nutrient concentration in the system; (c) growth rate of <i>Emiliania huxleyi</i> (red dots) and <i>Thalassiosira pseudonana</i> (green dots) according to the Monod model without cell death or wash-out and with a starting NO_3 concentration of 5 μM	40
Figure 14. (a) Cell density of <i>Emiliania huxleyi</i> (red solid line) and <i>Thalassiosira pseudonana</i> (green solid line); (b) nutrient concentration in the system; (c) growth rate of <i>Emiliania huxleyi</i> (red dots) and <i>Thalassiosira pseudonana</i> (green dots)	

according to the Monod model without cell death or wash-out and with a starting NO_3 concentration of 5 μM	41
Figure 15. (a) Cell density of <i>Emiliana huxleyi</i> (red solid line) and <i>Thalassiosira pseudonana</i> (green solid line); (b) NO_3 concentration in the system; (c) growth rate of <i>Emiliana huxleyi</i> (red dots) and <i>Thalassiosira pseudonana</i> (green dots) according to the Monod model (eq. 1) with a starting NO_3 concentration of 2 μM and a constant input of 2 μM	43
Figure 16. (a) Cell density of <i>Emiliana huxleyi</i> (red solid line) and <i>Thalassiosira pseudonana</i> (green solid line); (b) NO_3 concentration in the system; (c) growth rate of <i>Emiliana huxleyi</i> (red dots) and <i>Thalassiosira pseudonana</i> (green dots) according to the Monod model (eq. 1) with a starting NO_3 concentration of 0.8 μM , a constant input of 0.8 μMh^{-1} , and a dilution rate of 0.7.	44
Figure 17. (a) Cell density of <i>Emiliana huxleyi</i> (red solid line) and <i>Thalassiosira pseudonana</i> (green solid line); (b) NO_3 concentration in the system; (c) growth rate of <i>Emiliana huxleyi</i> (red dots) and <i>Thalassiosira pseudonana</i> (green dots) according to the Monod model (eq. 1) with a starting NO_3 concentration of 0.5 μM , a background input of 0.5 μMh^{-1} and a dilution rate of 0.7, a pulse period of 5 hours and a pulse length of 3 hours.	46
Figure 18. (a) Cell density of <i>Emiliana huxleyi</i> (red solid line) and <i>Thalassiosira pseudonana</i> (green solid line); (b) NO_3 concentration in the system; (c) growth rate of <i>Emiliana huxleyi</i> (red dots) and <i>Thalassiosira pseudonana</i> (green dots) according to the Monod model (eq. 1) with a starting NO_3 concentration of 0.5 μM , a background input of 0.5 μMh^{-1} and a dilution rate of 0.7, a pulse period of 13 hours and a pulse length of 5 hours.	47
Figure 19. (a) Cell density of <i>Emiliana huxleyi</i> (red solid line) and <i>Thalassiosira pseudonana</i> (green solid line); (b) NO_3 concentration in the system; (c) growth rate of <i>Emiliana huxleyi</i> (red dots) and <i>Thalassiosira pseudonana</i> (green dots) according to the Monod model (eq. 1) with a starting NO_3 concentration of 0.5 μM , a constant input of 0.5 μMh^{-1} and a dilution rate of 0.7, a pulse period of 24 hours and a pulse length of 6 hours.	48
Figure 20. (a) cell density of <i>Emiliana huxleyi</i> (red solid line) and <i>Thalassiosira pseudonana</i> (green solid line); (b) NO_3 concentration in the system; (c) growth rate of <i>Emiliana huxleyi</i> (red dots) and <i>Thalassiosira pseudonana</i> (green dots) according to the Monod model (eq. 1) with a starting NO_3 concentration of 0.5 μM , a background input of 0.5 μMh^{-1} and a dilution rate of 0.7, a pulse period of 120 hours and a pulse length of 15 hours.	49
Figure 21. (a) cell density of <i>Emiliana huxleyi</i> (red solid line) and <i>Thalassiosira pseudonana</i> (green solid line); (b) nutrient concentration in the system; (c) growth rate of <i>Emiliana huxleyi</i> (red dots) and <i>Thalassiosira pseudonana</i> (green dots) according to the Mixed Droop-Monod model without cell death or wash-out and with a starting NO_3 concentration of 5 μM	53
Figure 22. (a) cell density of <i>Emiliana huxleyi</i> (red solid line) and <i>Thalassiosira pseudonana</i> (green solid line); (b) nutrient concentration in the system; (c) growth rate of <i>Emiliana huxleyi</i> (red dots) and <i>Thalassiosira pseudonana</i> (green dots) according to the Mix Droop-Monod model with a starting NO_3 concentration of 2 μM , a constant input of 2 $\mu\text{M h}^{-1}$, and dilution rate of 0.7.	55

- Figure 23. (a) Cell density of *Emiliana huxleyi* (red solid line) and *Thalassiosira pseudonana* (green solid line); (b) nutrient concentration in the system; (c) growth rate of *Emiliana huxleyi* (red dots) and *Thalassiosira pseudonana* (green dots) according to the Mixed Droop-Monod model) with a starting NO_3 concentration of $0.8 \mu\text{M}$, a background input of $0.8 \mu\text{Mh}^{-1}$ and a dilution rate of 0.6, a pulse period of 5 hours and a pulse length of 3 hours. 56
- Figure 24. (a) Cell density of *Emiliana huxleyi* (red solid line) and *Thalassiosira pseudonana* (green solid line); (b) nutrient concentration in the system; (c) growth rate of *Emiliana huxleyi* (red dots) and *Thalassiosira pseudonana* (green dots) according to the Mixed Droop-Monod model) with a starting NO_3 concentration of $0.8 \mu\text{M}$, a background input of $0.8 \mu\text{Mh}^{-1}$ and a dilution rate of 0.6, a pulse period of 13 hours and a pulse length of 5 hours. 57
- Figure 25. (a) Cell density of *Emiliana huxleyi* (red solid line) and *Thalassiosira pseudonana* (green solid line); (b) nutrient concentration in the system; (c) growth rate of *Emiliana huxleyi* (red dots) and *Thalassiosira pseudonana* (green dots) according to the Mixed Droop-Monod model) with a starting NO_3 concentration of $0.8 \mu\text{M}$, a background input of $0.5 \mu\text{Mh}^{-1}$ and a dilution rate of 0.8, a pulse period of 24 hours and a pulse length of 6 hours. 58
- Figure 26. (a) Cell density of *Emiliana huxleyi* (red solid line) and *Thalassiosira pseudonana* (green solid line); (b) nutrient concentration in the system; (c) growth rate of *Emiliana huxleyi* (red dots) and *Thalassiosira pseudonana* (green dots) according to the Mixed Droop-Monod model) with a starting NO_3 concentration of $0.8 \mu\text{M}$, a background input of $0.8 \mu\text{Mh}^{-1}$ and a dilution rate of 0.6, a pulse period of 120 hours and a pulse length of 20 hours. 59

List of tables

Table 1. Symbols used in models of resource competition and their units.....	6
Table 2. <i>Emiliana huxleyi</i> general characteristics	17
Table 3. General characteristics of <i>Thalassiosira pseudonana</i>	22
Table 4. Parameters set for the Monod model	38
Table 5. Parameters set for the Mixed Droop-Monod model	51

1 Introduction

"The biotas of pelagic ecosystems are far too complex to be analyzed species by species."

Bruce Frost 1984

Observed variations in phytoplankton community composition are driven by the synergistic interactions between physical, biological, and chemical processes [Margalef, 1960 #350]. The net result of these synergistic interactions is to maintain a high phytoplankton diversity [Smayda, 1980 #347] and references therein). Given this, a fundamental question for oceanographers is to understand how key environmental factors select for a particular phytoplankton assemblage and to understand the potential impact on the biogeochemical cycling of elements in the oceans [Falkowski, 1998 #354; Hedges, 1992 #566]. For example how is carbon and silica cycling in the oceans impacted by a shift from silicifying diatoms to calcifying coccolithophores. Phytoplankton community dynamics has been related to many chemical and physical parameters which all operate over a range of space and time scales (Daly and Smith 1993). It is well known that phytoplankton production is regulated by a combination of factors such as light (Kirk 1983; Litchman and Klausmeier 2001; Mitchell et al. 1991; Morel 1978; Peterson et al. 1987; Platt and Jassby 1976), temperature (Arrigo and Sullivan 1992; Cloern 1977; Eppley 1972; Goldman and Ryther 1976; Li 1985), macronutrients such as nitrogen and phosphate (Hein and Riemann 1995; Raven 1997; Riegman et al. 2000) and silica (Dugdale and Wilkerson 1998; Egge and Aksnes 1992; Paasche 1973; Walsh 1971) and micronutrients such as iron (Banse 1995; Martin 1992). The relative impact of each these

environmental variables on the community dynamics will be determined by the physiological capacity of phytoplankton to maximize growth under a given condition. (Margalef 1960)

Therefore my research has focused on understanding the physiological-forcing of phytoplankton community dynamics between marine diatoms and coccolithophores. I have formulated a simple numerical prognostic competition model for these two taxa in order to study how their bloom dynamics is impacted by nutrient availability. More specifically I have studied how different nutrient pulse frequencies and durations impact the competition and succession of coccolithophores and diatoms.

My main hypothesis is that nutrient pulses with different frequency, length and intensity, regulate the abundance, dominance, and succession of coccolithophores and diatoms. This is an extension of the intermediate disturbance hypothesis (Connell 1978), and the physical disturbance hypothesis comparable to Margalef's phytoplankton "mandala" (1978) that proposes water column mixing (Figure 1) and turbulence (Figure 2) regulate phytoplankton community composition and succession (Lewis et al. 1984; Margalef 1997).

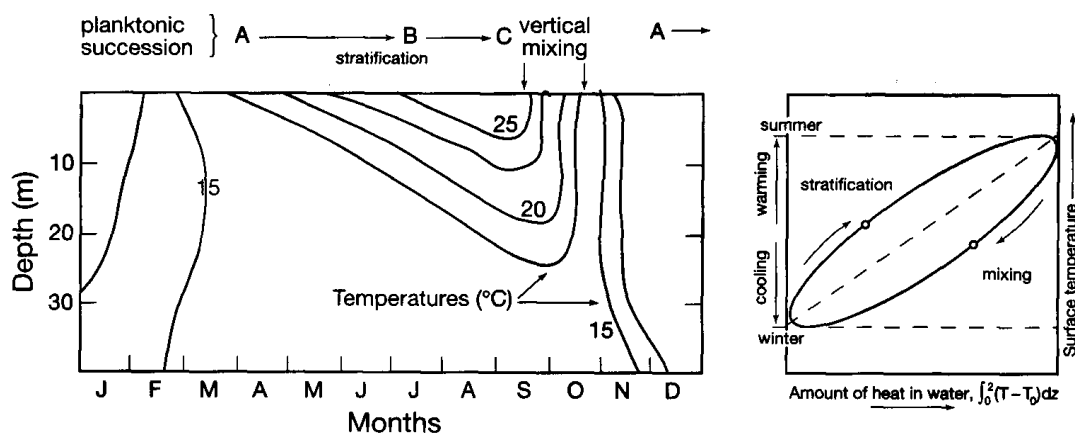


Figure 1. Alternation between successional dynamics and discontinuous resetting. On the left water column thermocline variation during a year in relation to planktonic succession. On the right seasonal variation of water temperature, mixing, heat amount in water and energy. From (Margalef 1997)

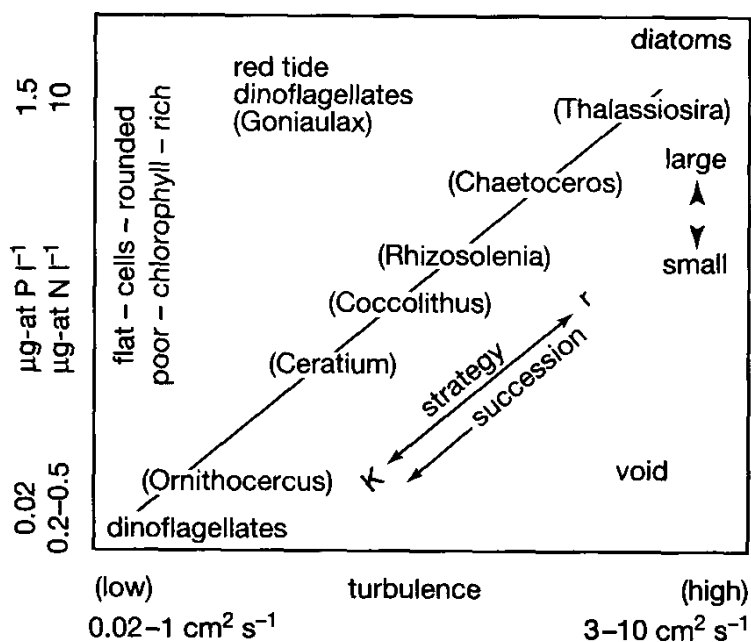


Figure 2. The phytoplankton "mandala". Dominance and succession of different phytoplankton organism it is explained with a correlation between different combinations of environmental factors. From (Margalef 1997)

I hypothesize that diatoms will an advantage when turbulent mixing maintains high nutrient concentrations into the euphotic zone, while coccolithophores are positively selected under more stable conditions when nutrient fluxes are low during periods of stratification. This is based on diatoms having storage vacuoles and high nutrient uptake capacities (Raven, 1997), while coccolithophores lack storage vacuoles and have lower nutrient uptake rates (Eppley et al., 1969; Riegman et al., 2000). Given this, we have focused our efforts to understand how the succession of diatoms and coccolithophores is driven by the concentration of nitrate. The appropriateness of considering nitrate alone is reasonable as biologically-useable nitrogen, limits ocean primary production over annual and geologic timescales (Ryther 1956).

My prognostic model simulates diatoms as having a Droop-type physiology (Droop 1973), which describes the growth rate as a function of the extracellular and intracellular concentration of the limiting nutrient, while coccolithophores growth more closely follows a Monod type of physiology, which is dependent on the extracellular substrate concentration. These model results were combined with laboratory measurements that allowed me to parameterize and initialize the numerical simulations. The modeling philosophical goals, modeling approaches, and physiological profiles for the test organisms are outlined below.

1.2 Succession and resource competition: theory and related algal growth models

Descriptive models of interspecific competition were first developed as the logistic equation of Pearl and Reed in 1920 and revised to the Lotka and Volterra model in 1925 and 1926. This model can be used to study the competition coefficient and the carrying capacities of the algae in terms of rates of utilization and renewal of resources (Morin 1999). Given this, the model describes not only the interaction between species but also the interaction between consumers and external resources.

To test the effects of different frequency of nutrient pulses on the competition between diatoms and coccolithophores, two mechanistic models were used (a Monod model and a mixed Droop-Monod model). The Monod model implicitly assumes that growth rate is regulated exclusively by extracellular nutrient concentration. This is appropriate for coccolithophores that lack nutrient vacuoles. For the diatoms, which containing vacuoles, a mixed model was adopted, using Monod type kinetics for the coccolithophore and a variable internal store (VIS) based on the Droop equation (Droop 1973). In general, more frequent pulses should be advantageous for diatoms, which have a fast uptake rate, a higher half saturation constant; and the vacuoles that allow these organisms to maintain a higher growth rate between nutrient short pulses. With less frequent nutrient pulses, the high affinity coccolithophores have assimilating nitrogen will provide them a competitive advantage under low nutrient conditions (Eppley et al. 1969). A more detailed model description is provided below. Table 1 reports the symbols of the variables used in the two models, which will be successively introduced.

Table 1. Symbols used in models of resource competition and their units

Symbol	Units	Meaning
State variables:		
N	cell L ⁻¹	Population density
R	μmol L ⁻¹	Resource availability
Q	μmol cell ⁻¹	Cell quota
Physiological functions:		
μ	h ⁻¹	Growth rate
ρ	μmol cell ⁻¹ h ⁻¹	Uptake rate
Parameters:		
D	h ⁻¹	Dilution rate
R^0	μmol L ⁻¹	Constant nutrient inflowing rate
Y	cell μmol ⁻¹	Cell yield constant
μ_{max}	h ⁻¹	Maximal growth rate
K_i	μmol cell ⁻¹	Growth rate half saturation constant
Q_0	μmol cell ⁻¹	Minimal cell quota
Q_{max}	μmol cell ⁻¹	Maximal cell quota
K_ρ	μmol L ⁻¹	Half saturation constant for uptake
Notational conventions:		
i		Subscript to distinguish terms pertaining to a given species
t	h	Time

1.2.1. Monod model

The Monod model describes phytoplankton growth as a function of dissolved extracellular nutrient concentration. Monod (Monod 1950) first applied this model to describe bacteria growth rate based on two simple parameters, substrate (R) and growth rate (μ). He found a hyperbolic function between the two, and adopted the Michaelis-Menten equation for enzyme kinetics to describe this relation between substrate and growth rate. In this model, the cell growth rate is given by the following equation (Eq. 2)

$$\frac{dN_i}{dt} = \left(\frac{\mu_{\max_i} \cdot R}{K_i + R} \right) \cdot N_i - D \quad (\text{Eq. 1}).$$

and the resource consumption is given by

$$\frac{dR}{dt} = D(R^0 - R) - \sum \frac{N_i \mu_{\max_i} R}{Y_i (K_i + R)} \quad (\text{Eq. 2})$$

where N is the cell density of the i^{th} species, μ_{\max} is the maximum growth rate achievable when the concentration of the growth-limiting nutrient R is not limiting, K_i is the concentration of the growth-limiting nutrient at which the specific growth rate is half the maximum value. K_i represents the affinity the organism has for the nutrient. D is the death (dilution) rate of the organism considered (Monod, 1950). An example of the specific growth rate against the concentration of the growth-limiting nutrient is shown in Figure 3. For the run presented in Figure 3, NO_3 is the limiting nutrient and the diatoms and coccolithophores are the two organisms. These are parameterized in Table 4. This model illustrates the immediate response of the cell growth rate to the external resource concentration. The change in population density results as a balance between the growth rate and the dilution rate.

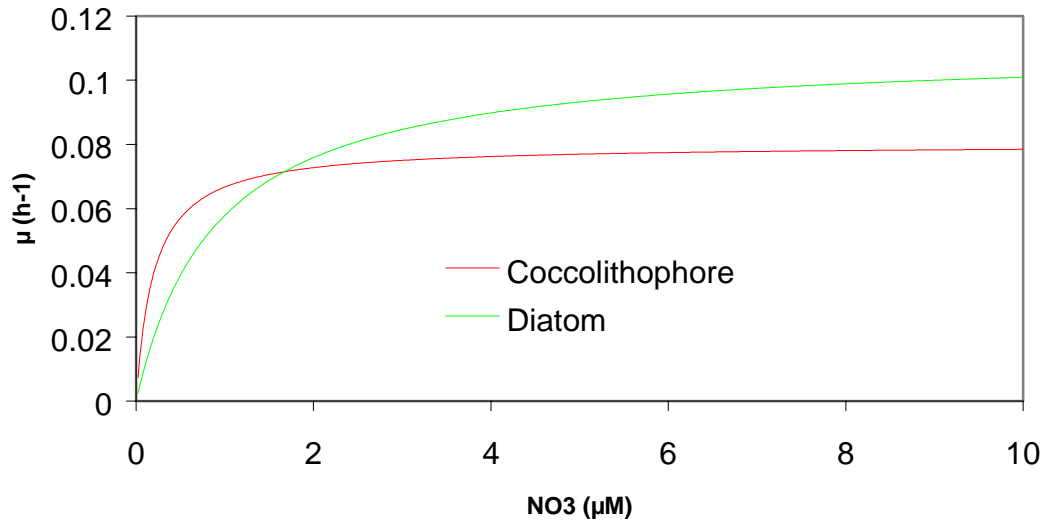


Figure 3. Growth function for *Emiliania huxleyi* (red line) and *Thalassiosira pseudonana* (green line) according a Monod model. The two organisms are parameterized as described in (Table 4).

When equilibrium is reached between loss and growth rates, there will be a superior competitor, which has the smaller resource requirement (R_i^*) (Tilman 1977).

$$R_i^* = \frac{DK_i}{\mu_{\max i} - D} \quad (\text{Eq. 3})$$

This parameter can be used as a predictor of the competitive outcome at equilibrium and in absence of competitors (Grover 1989). The prediction given by R^* may change if the system does not reach an equilibrium, as in the case of a variable resource supply.

1.2.2. Droop model

In the late 1960's, Droop introduced the use of chemostats to limnology and biological oceanographic studies. The Droop model is derived by an empirical relation of a specific growth rate in a steady state system to the nutrient status (Droop 1973). Droop formulated his model studying the effect of vitamin B₁₂ on phytoplankton growth rate. The Monod model was not sufficient to explain the relationship between growth rate and external concentration of vitamin B₁₂, but by introducing a term for cell quota and using equation 5, the growth rate could be modeled based on B₁₂ concentrations. This model is based on the assumptions that the uptake of the resource (ρ) in steady state is a function of the growth rate and the internal nutrient concentration (Q) (Eq.7).

Under nutrient-limited conditions, there appears to be little relationship between algal growth rates and extracellular nutrient concentrations for the same species. Due to mobilization of intracellular pools, growth rates can be more closely related to the sum of intracellular nutrient pools and storage (often referred to as the cell quota, Eppley and Strickland, 1968). When intracellular storage is exhausted and intracellular nutrient pools are at minimal levels, growth rates are regulated by the external rate of supply of the limiting nutrient. When supply rates and growth rates are closely coupled under nutrient depletion, there may be a less clear relationship between the extracellular nutrient concentrations and algal growth rates due to continuous uptake by nutrient- starved algae (Fisher and Butt 1994).

The effects of extracellular nutrient concentration and cell quota on algal growth rates can be summarized as follows:

$$\mu = \mu_{\max} \cdot \left(\frac{1 - k_Q}{Q} \right) \quad (\text{Eq. 4})$$

This equation was modified by (Caperon and Meyer 1972), who found that growth rate was better modeled by taking into account the difference between the cell quota (Q) and the minimal cell quota (Q_0) when considering macronutrients.

$$\mu = \frac{\mu_{\max} (Q - Q_0)}{k_Q + (Q - Q_0)} \quad (\text{Eq. 5})$$

$$\rho = \mu \cdot Q \quad (\text{Eq. 6})$$

μ indicates the growth rate, μ_{\max} represent the maximal cell division rate, Q is the cell quota for a given nutrient, Q_0 is the minimal cell quota, k_Q is the half saturation constant for cell division and ρ is the uptake rate. ρ can also be expressed as a function of the maximal uptake, substrate concentration, and half saturation constant.

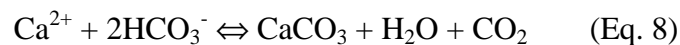
$$\rho = \frac{\rho_{\max} \cdot R}{K_r + R} \quad (\text{Eq. 7})$$

The presence of intracellular storage (e.g. a vacuole) introduces a time lag between the exhaustion of the extracellular nutrient concentration and the actual nutrient limitation of growth. As the extracellular pool becomes smaller, intracellular storage and pools are

reduced; there will be a time delay between depletion of the extracellular pool of the limiting nutrient and the reduced rate of growth.

1.3 Phytoplankton functional groups

The functional group concept is based on the idea that in all ecosystems, certain organisms have significant biogeochemical and ecological roles. Within the notion of functional group then, organisms can be related through common biogeochemical processes rather than phylogenetic affiliation. In the case of oceanic diatoms, these are the most successful group and major contributors to the global ocean primary production in the modern ocean, account for approximately 40% of the global annual primary production (Falkowski and Raven 1997). Given this, they occupy a key position in regulating the carbon dioxide flux and biological pump (Longhurst and Harrison 1989). At the same time, they convert soluble ortho silicic acid to solid hydrated amorphous opal (Busby and Lewin 1967; Paasche 1973; Sullivan 1976; Sullivan 1977). In contrast coccolithophores calcify; they convert dissolved inorganic carbon and calcium to solid phase calcite and aragonite (Young et al. 1991) (Eq. 1) altering the equilibrium of the inorganic carbon system and alkalinity of seawater according to [Holligan, 1996 #749; Denman, 1999 #745]



To put coccolithophores in perspective in the contemporary ocean *Emiliania huxleyi* forms seasonal blooms that globally represent the single largest source of biogenically produced calcite (Westbroek et al., 1989), and accounts for 20-30% of the total calcium carbonate buried in the ocean ([Broecker, 1982 #743]; Honjo et al., 1982). On a short time scale, calcification leads to an imbalance in the carbonate system and increases the carbon dioxide flux from the ocean to the atmosphere. Over geological time the system can be brought back to a steady state by adjusting the lysocline depth and the calcium carbonate burial time (10³-10⁴ y). Rock weathering restores alkalinity by adding free calcium on longer time scales of about a million years. Given that free calcium residence time is longer than a million years, the short-term changes in alkalinity can significantly affect the global carbon cycle (Quay, 1992; Heimann and Maier-Reimer, 1996; Joos and Bruno, 1998).

1.4 Coccolithophores

Emiliana huxleyi (Figure 4) is the most abundant coccolithophore in the modern ocean. Coccolithophores shield their cells with calcium carbonate platelets, named coccoliths. This species belongs to the Prymnesiophytes family, which evolved in the mid-Triassic [Lipps, 1993 #751].

Emiliana huxleyi is spherical, with a diameter of about 5 μm . The small dimension provides an advantage in stratified, oligotrophic waters by the high surface to volume ratio, which enhances nutrient diffusion and nutrient uptake at low concentrations.

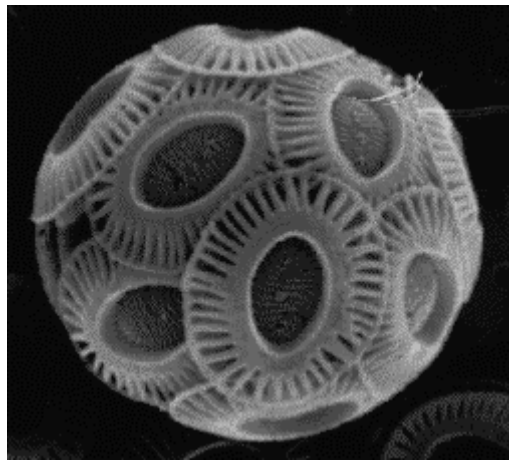


Figure 4. SEM photography of *Emiliana huxleyi* (<http://www.soc.soton.ac.uk/SUDO/tt/eh/>)

This species is globally distributed and in favorable conditions can form massive bloom, reaching extensions up to 100,000 km^2 of ocean surface [Brown, 1994 #758].

Coccoliths distinguish *Emiliana huxleyi* from other prymnesiophytes. They have an important role in the sinking rates of *Emiliana huxleyi* that is not a motile cell, and they

can be used as ballast. Coccolithophores can in fact vary their sinking rate by detaching or producing the platelets [Eppley, 1967 #746]. Under high nutrient conditions a loss of coccoliths has been reported by Klaveness and Paschee (1979). The opposite phenomenon, high calcification under low nutrient concentrations, allows the cells to sink faster and reach deeper nutrient rich waters, while enhancing nutrient diffusion at the same time (Wilburn and Watabe 1963, [Linschooten, 1991 #537]). Other proposed functions for coccoliths are to act as protection from parasites and predators (Paasche 1967) Young, 1994).

From an evolutionary point of view, calcium carbonate platelets are an optimum solution in comparison to silicate, cellulose or other organic polymers. The reason for this is that calcium carbonate platelets are energetically less costly than organic polymers, which require carbon dioxide reduction by NADPH (Brand 1994). The silica necessary for diatom frustules is at a limiting concentration in most ocean photic zones, whereas calcium carbonate is at a supersaturating concentration in tropical and temperate photic zones [Broecker, 1982 #743].

1.4.1. Biology and physiology

Emiliana huxleyi can live in a wide range of temperatures, from 1 to 31 °C (McIntyre et al., 1970). In reality, there are many different clones of the same species that are adapted to different portions of this wide temperature range. *Emiliana huxleyi* clones isolated from the Sargasso Sea showed higher growth rates, between 18 and 24 °C (Watabe and Wilburn 1966), are genetically different from the clones isolated in the cold waters of the Gulf of Maine (Brand 1982) adapted to lower temperature, and from those isolated from coastal waters south of Cape Cod (Fisher and Honjo, 1991).

Emiliana huxleyi has a broad salinity range, from 41 ppt in the Red Sea (Winter et al., 1979), to 11 ppt in the Black Sea (Bukry, 1974).

In contrast with other coccolithophores, *Emiliana huxleyi* is the only species slightly inhibited by continuous light [Brand, 1981 #621]. Laboratory and field productivity vs. irradiance (PI), curves in which *Emiliana huxleyi* was acclimatized to and tested at high light intensities, do not become photo-inhibited, even at the highest light intensities likely to be encountered in nature [Nanninga, 1996 #691]. This lack of photoinhibition may be a reason underlying their apparent success at high light. The photoperiod of *Emiliana huxleyi* has shown a strong dependency on calcification. *Emiliana huxleyi* divides primarily during the dark (Nelson and Brand 1979), and its N-assimilating enzymes, nitrate reductase and nitrite reductase, showed higher activity during the light period of the cycle (Eppley et al. 1971).

(Eppley et al. 1969) reported half saturation constants for nitrate and ammonium uptake for 16 species of phytoplankton. They found there was a strong adaptation of *Emiliana*

huxleyi to low nutrient conditions. Similarly, *Emiliana huxleyi* also has a low iron requirement [Brand, 1991 #7296].

Emiliana huxleyi can use both inorganic and organic forms of phosphorous because it can hydrolyze the latter by a phosphatase present on the cell surface [Riegman, 2000 #673]. *Emiliana huxleyi* also requires thiamine (Carlucci and Bowes 1970). As most coccolithophores, *Emiliana huxleyi* reproduction is by asexual binary fission. This specie can divide up to 2.5 times a day (Brand and Guillard 1981). Table 2 reports the main biological and physiological features of this organism.

Table 2. *Emiliania huxleyi* general characteristics

Parameter	Units		Reference
Cell diameter	μm	4-8 4	Present work [♦] (Tyrrell 2000)
Cell volume	μm^{-3}	30-260 35-60	Present work [♦] (Muggli and Harrison 1996; Payne and Price 1999)
μ_{max}	d^{-1}	1.9-2.5 0.3-2.6	Present work [♦] (Muggli and Harrison 1996; Nelson and Brand 1979)
Chl <i>a</i> cell ⁻¹	pg cell^{-1}	0.12 ± 0.06 0.04-0.29	Present work [♦] [Muggli, 1996 #536; Fernández, 1996 #663]
Temperature range	$^{\circ}\text{C}$	1-31	(McIntyre et al., 1970)
N cell ⁻¹	pg cell^{-1}	1.9 ± 0.1 1.4-5.6	Present work [♦] (Muggli and Harrison 1996; Payne and Price 1999)
$^{\diamond}\text{C}_t$ cell ⁻¹	pg cell^{-1}	31 ± 0.8 10-32	Present work [♦] (Muggli and Harrison 1996; Muggli and Harrison 1997)

[♦]Cells grown in f/2 at 18°C, in continuous light 150 $\mu\text{E m}^{-2} \text{s}^{-1}$ CCMP 0374

[♦] C_t it is the is the total carbon including the coccolith carbon.

1.4.2 Diversity and biogeography

Coccolithophores appear to be more diverse and ubiquitously distributed in the Cretaceous (146-65 mya) geological records than at present time (Tappan, 1980). These derive as shown in (Figure 6) from a secondary endosymbiosis that gave rise to the photosynthetic stramenopiles (including diatoms, chrysophytes, and brown algae that occurred over a billion years ago [Knoll, 1996 #8095]. In the modern ocean, the highest

diversity of coccolithophores is found in the subtropical oceanic gyres (Hulburt, 1963, Haidar, Thierstein et al. 2000). In temperate and subpolar waters higher abundance is found but this coincides with lower diversity (Hulburt, 1963). Also in coastal waters, there are fewer number of coccolithophores species found, but they are never a dominant component of the community in this environment.

Most coccolithophores today are found in warm, stratified, nutrient poor offshore waters, and prevail over other species in temperate waters only during the spring and summer. They are permanently present in tropical waters. There are some cases where *Emiliana huxleyi* becomes very abundant in nutrient rich waters (Balch et al. 1996a; Balch et al. 1996b). This phenomenon happens along the edges of subtropical central gyres, in upwelling regions and on the outer portion of continental shelves. (Brand 1994). Distribution of *Emiliana huxleyi* based on satellite data is shown in Figure 5.

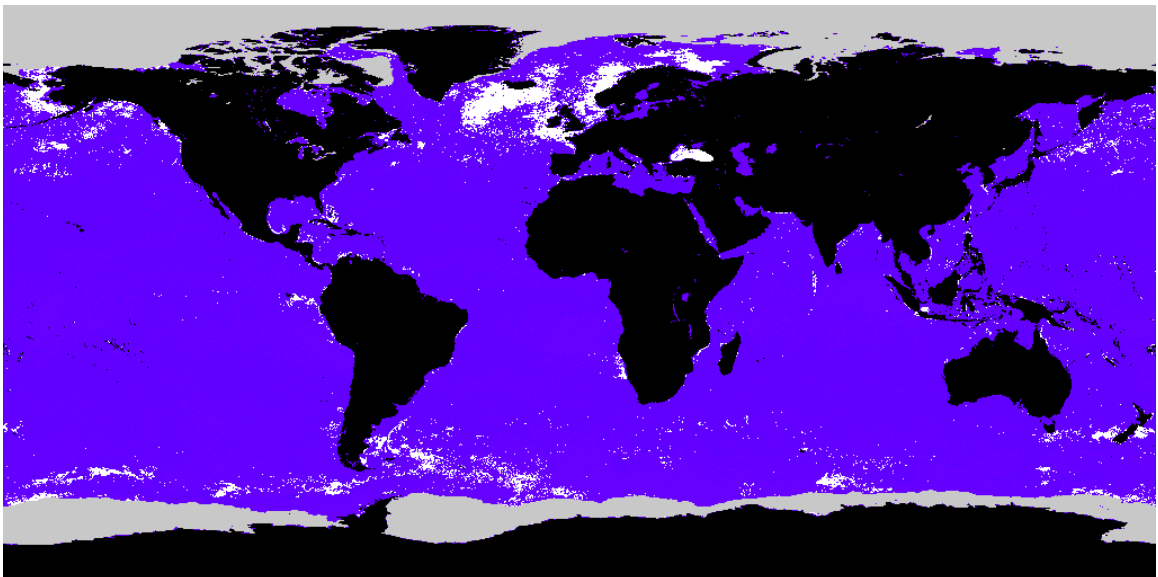


Figure 5 Annual composite of classified coccolithophore blooms in SeaWiFS imagery dating from October 1997 to September 1999. The bloom class is white, the non-coccolithophore bloom class is blue, the land is black and the ice is gray

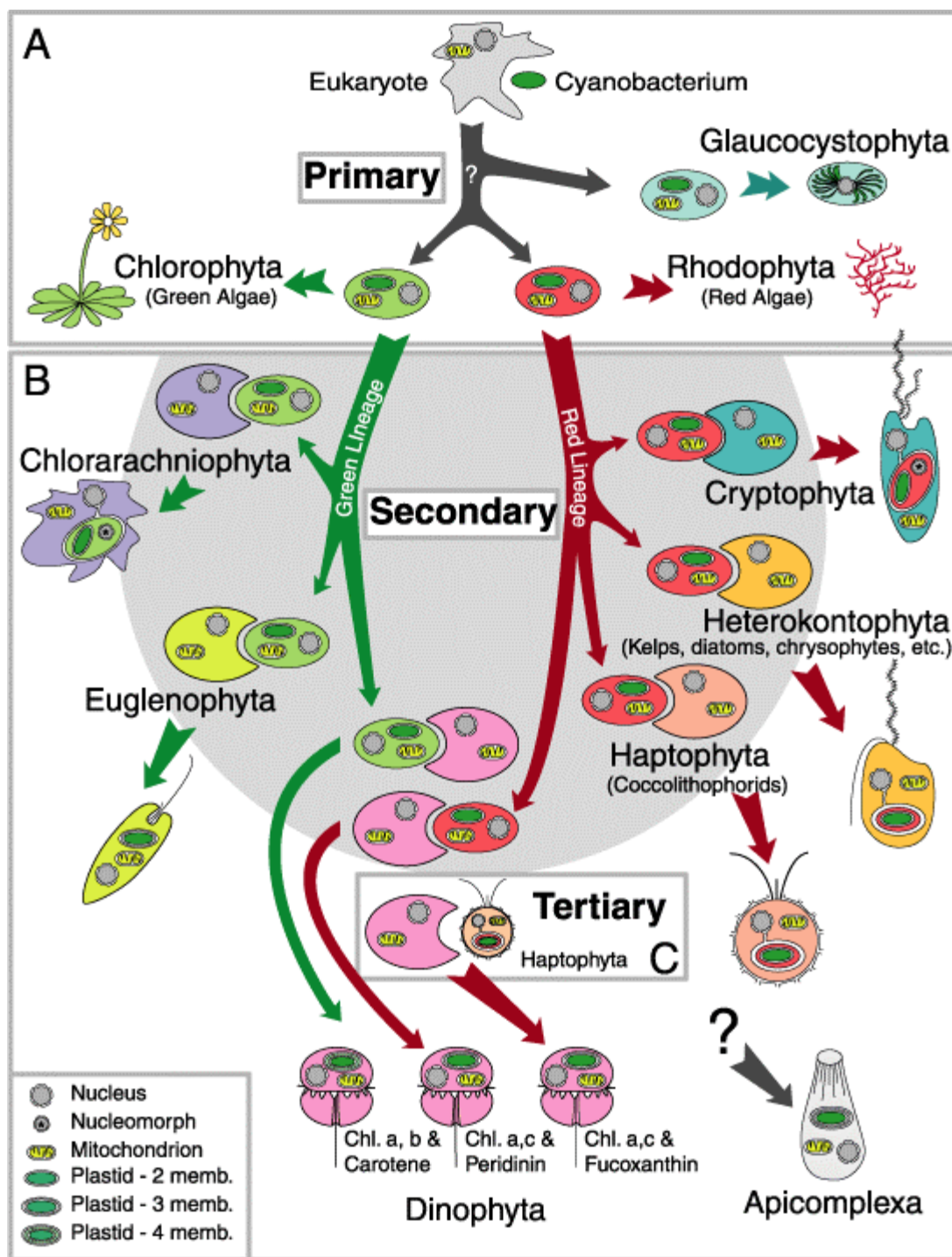


Figure 6. Evolution of the major eucaryotic phytoplankton taxa from Delwiche (1999)

1.5 Diatoms

Diatoms belong to the class Bacillariophyceae and division Chromophyta. As Prymnesiophytes diatoms derive from a secondary endosymbiosis (Figure 6). There are 10,000 extant diatom species of which half are marine (Falkowski and Raven 1997). These can range in diameter from about 2 μm to over 1000 μm . Some species form colonies and/or aggregates in which mucilage or spines hold single cells together. All species are characterized by siliceous frustules. Diatoms have a variety of strategies to keep them in the euphotic zone and regulate their buoyancy. These range from morphological features, cell surface to volume ratios and vacuoles' ionic regulation. All these can change the frictional drag of the cells determining different sinking rates. Sinking rates vary from 0 to 30 m a day (Bienfang 1985; Bienfang et al. 1982).

For the present work, *Thalassiosira pseudonana* was chosen as a model organism representative of diatoms, even though different species of diatoms and different clones of the same species can present a wide range of different physiological attributes. The reason for choosing this particular species is primarily due to its size, which matches the size of *Emiliana huxleyi*. This allows one to consider the difference in physiological responses, which do not have to be size dependent.

1.5.1 Biology and physiology

Reproduction in diatoms is usually by asexual division leading to fast growth. As diatoms reproduce, they generate smaller and smaller cells until they reach a critical minimal size then they need to reproduce sexually, and a small zygote enlarges to form an auxospore. *Thalassiosira pseudonana* in a 14:10 LD cycle showed two peaks in division, one in the middle of the light, another in the middle of the dark period (Brzezinski 1985; Chisholm et al. 1980).

(Paasche 1980) showed a temperature dependence in variation of Si:C in *Thalassiosira pseudonana*, with a higher ratio of 0.23 (gSi/gC) at the higher temperature of 25 °C. In a continuous Si-limited culture, *Thalassiosira pseudonana* produced a hyperbolic relationship between the growth rate and Si content (Paasche 1973). (Olsen and Paasche 1986) instead suggested that there is no simple mathematical expression that connects the growth rate and Si quota. In these experiments the growth was light saturated at 20 °C with 170 µE. The cell's C and N accumulates during the daylight as division proceeds at low rate, while silica accumulates just prior to division bursts, because diatoms can not store sufficient silicon for new valve formation (Azam, 1974; (Sullivan 1977); Binder, 1980). Data from (Brzezinski 1985) suggests that the net effect of the photoperiod on the Si:C:N composition of diatoms over diurnal period is small and not distinguishable from the one of culture grown at constant light. The Si:C:N ratio can be effected from temperature and nutrient limitation. Overall, silica limits distribution of diatoms and abundance in the global ocean. In Table 3, the main biological and physiological features of this organism are reported.

Table 3. General characteristics of *Thalassiosira pseudonana*

Parameter	Units		Reference
Cell diameter	μm	3-6 4-6	Present work [♦] CCMP*
Cell volume	μm^3	95-115 95-136	Present work [♦] (Brzezinski 1985)
μ_{max}	d^{-1}	0.7-2.9 0.7-4.8	Present work [♦] (Brand and Guillard 1981; Davidson et al. 1999)
Chl <i>a</i>	pg cell^{-1}	0.22 ± 0.5 0.13-0.33	Present work [♦] (Sakshaug et al. 1987)
Temperature range	$^{\circ}\text{C}$	4-25	CCMP*
N cell ⁻¹	pg cell^{-1}	10.64	(Brzezinski 1985)
C cell ⁻¹	pg cell^{-1}	50	(Brzezinski 1985)
Si cell ⁻¹	pg cell^{-1}	5.88	(Brzezinski 1985)

*Provasoli-Guillard National Center for Culture of Marine Phytoplankton (CCMP)

database

[♦]Cells grown in f/2 at 18°C, in continuous light 150 $\mu\text{E m}^{-2} \text{s}^{-1}$ CCMP 1335 clone 3H

1.5.2 Diversity and biogeography

Diatoms are globally distributed, and in nutrient rich environments often dominate community structure. The global distribution of diatoms can be derived by annual production of opaline in the world ocean (Figure 7) (Bishop 1989).

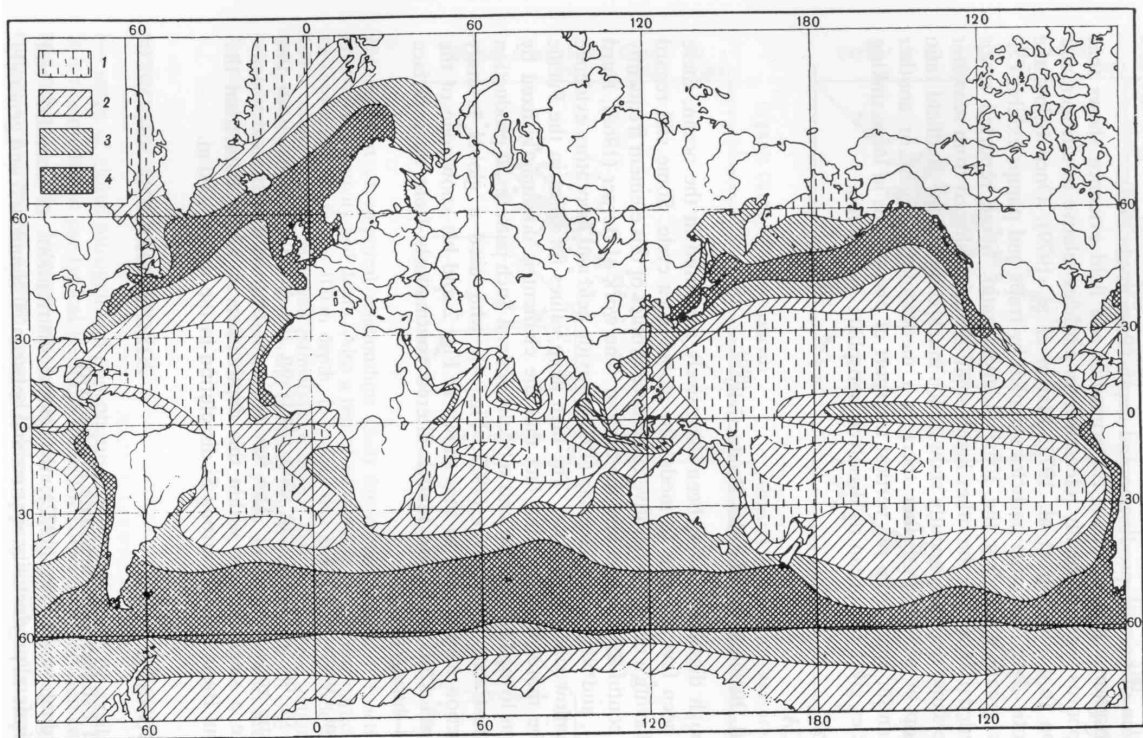


Figure 7. Annual production of opaline silica in the world ocean ($\text{g Si}_2 \text{ m}^{-2} \text{ y}^{-1}$) (from Lisitzin, 1972). Key: 1= <100; 2= 100-250; 3=250-500; 4=>500. The cross-hatched area at 15°S and 180°W is from a printing error in early primary productivity maps and should be <100 (see Berger et al 1987, p.49).

Diatoms have been abundant in the ocean since the Jurassic (160 mya) and lower Cretaceous (100 mya), and diatomaceous ooze deposits are records of their abundance over geological times (Harwood and Gersonde, 1990).

2 Material and Methods

Experiments were performed on diatoms and coccolithophores grown in semicontinuous or batch cultures. The two organisms were *Thalassiosira pseudonana* (Bacillariophyceae) CCMP 1335, clone (3H), and *Emiliana huxleyi* (Prymnesiophyceae) CCMP 374. These two organisms were chosen because they have the same cell size, thereby avoiding size dependent nutrient uptake, carbon fixation and growth rate responses. The cultures have been maintained and were kept under continuous light $150 \mu\text{E m}^{-2} \text{ s}^{-1}$ to have unsynchronized growths. The two organisms were cultured in f/2 media or derivatives as f/10 and f/2 with a nutrient Redfield ratio (Guillard 1975; Guillard and Ryther 1962). The cultures were bubbled with air and stirred with magnetic stirrers to keep cells in suspension.

2.1. Growth rates and cell size

For all experiments, live samples were counted with a Beckman Coulter Multisizer II particle size analyzer [Parson, 1973 #570]. A $70 \mu\text{m}$ aperture tube was used and measurements were made on a $500 \mu\text{L}$ sample. For the competition experiments and some time in concomitance of *in vivo* sampling, fixed samples (with Lugol's iodine solution) were collected and stored in the dark, and counted with a hemacytometer slide and a Zeiss Axioplan microscope with a 40X objective no later than ten days after fixation. A minimum of a 100 cells was counted for each sample.

2.2. Chlorophyll *a*

Duplicate samples of pigments samples were collected by filtration on Whatman GF/F Glass Microfiber Filters. The filters were stored at -20 °C until the end of the experiment, and then used to extract chlorophyll *a*. Chlorophyll *a* was extracted in a 90% acetone solution (Strickland and Parsons 1972) with the aid of a mechanical tissue grinder, and was allowed to steep for a minimum of 2 hours, and a maximum of 24 hours in the dark at 4 °C to ensure a thorough extraction. The filter slurry was centrifuged at 1000 g for 5 minutes to clarify the solution. An aliquot of the supernatant was transferred to a glass cuvette and absorbance was measured using an AMINCO DW2000 spectrophotometer. The pigment concentration was then computed as described by Jeffrey and Humphrey (1975).

2.3 Fast Repetition Rate (FRR) fluorescence

Variable fluorescence was measured on 1 mL of *in vivo* samples with a bench Fast Repetition Rate fluorometer (FRR) (Kolber et al. 1998). The sample was dark-adapted for about a minute and then successively measured. F_m indicates the maximum fluorescence level of Chl *a* fluorescence measured after dark-adaptation. F_0 indicates the minimum fluorescence level of Chl *a* fluorescence measured after dark adaptation. F_v indicates the variable fluorescence and is the difference between the maximum and minimum fluorescence level of Chl *a*. The benchtop FRR was used to measure the maximum quantum yield of photochemistry in Photosystem II (F_v/F_m). The FRR

technique applies a sequence of subsaturating excitation pulses at microsecond intervals to induce fluorescence transients, generating a single turnover and multiple turnover flashes

2.4 *Emiliana huxleyi* N cell quota

Samples for CHN analysis were collected on 13 mm Whatman GF/F Glass Microfiber Filters, precombusted at 375° for 12 hours. Ten mL samples were run through a syringe with a swinex containing the precombust filter. Following filtration, clean forceps were used to transfer each filter to a clean aluminum foil involucres. The sample was labeled and stored frozen at -20°C. CHN was measured with a PerkinElmer 2400. Standard procedures for instrument warm-up were followed. Primary PC/PN standards were prepared using acetanilide (C_8H_9NO ; mol. wt. = 135.16). Filters were packed in a standard tin capsule and dried in a dessicator for 24 hours before analysis (Sharp, 1974). Blanks were prepared by analyzing combusted GF/F "experiment filters" and the mean value subtracted from the sample value. Tin capsule blanks were run for every 5 samples.

2.5 *Nutrients*

Nitrate, phosphate and silicate were measured for the competition experiment, and nitrate was also measured for an *Emiliana huxleyi* nitrate uptake experiment. All the nutrients were measured with a Lachat Quick Chem Autoanalyzer following a modified

(Grasshoff 1976) protocol. More specifically standard autoanalyzer methods were used such as the Lachat QuickChem Method 31-107-04-1-A for NO_3 , Lachat QuickChem Method 31-115-01-3-A for PO_4^{3-} and Lachat QuickChem Method 31-114-27-1-A for SiO_2 . Sterile sampling procedures were used throughout the experiments. Ten mL samples were filtered through Whatman GF/F Glass Microfiber Filters, and collected in BLUE MAX JR. disposable centrifuge tubes, polystyrene, and frozen at -20°C . Check standards were run for every 9 samples, and they always gave a result within 5% of the expected value.

2.6 *Emiliana huxleyi* nitrate uptake

Six different treatments (200, 100, 50, 25, 12.5, 6.3 μM of NO_3) with three replicates each were prepared to measure nitrate uptake in *Emiliana huxleyi*. At time zero, 250 mL Erlenmeyer flasks were inoculated with 1 mL of culture with a cell density of 10^6 cell/mL. These were sampled at 0, 5, 15, 30 and 60 minutes. Ten mL samples were filtered and analyzed as described in section 2.5.

2.7 Competition experiment

Two monospecific batch cultures, one of *Thalassiosira pseudonana* and the other of *Emiliana huxleyi*, and one mixed batch culture were grown in a one liter Erlenmeyer Polycarbonate Flask (NALGENE) to avoid Si contamination. A modified f/2 media with a N:P 16:1 ratio was used. The cultures were bubbled with air and stirred with magnetic stirrers, to keep cells in suspension. Cultures were kept in continuous light at 18 °C. Daily sampling and measurements included: cell counts, variable fluorescence, chlorophyll determination, and nutrients.

2.8 Numerical simulation

To develop the numerical simulations, Matlab 6 ® software package was used. A Monod model (equations 1 and 2) and a mixed Droop-Monod based model (equations 4

and 6) were parameterized using data from earlier literature and present laboratory experiments (Table 4, Table 5).

The set of differential equations for the cell density and nutrient concentration over time in the Monod model, and the cell density, nitrate cell quota in diatoms and nitrate concentration over time in the Droop model were all solved with the Matlab implemented solver ode15s. The ode15s is a variable order solver based on numerical differentiation formulas, and is a multi-step solver for stiff problems. A pulse function (puls1.m in appendix) was created to smooth the nutrient pulse, and a tenfold amplification of the time step is implemented in the code for the same purpose. All runs were initialized with 1000 cells for each species. The simulation of competition in the batch culture and continuous resource supply were run for 300 model hours. This was the time necessarily to stabilize the system. The simulation of competition with pulsed resource supply were run for 1000 model hours, to verify the effect of the resource variable regime and allow at least 8 pulses with a 120 hours period pulse test.

3 Results

3.1 *Emiliana huxleyi* and *Thalassiosira pseudonana* growth rates and variable fluorescence

Semicontinuous cultures of *Emiliana huxleyi* and *Thalassiosira pseudonana* were grown and monitored. The maximal growth rate registered for *Thalassiosira pseudonana* was 2.88 (d^{-1}), which corresponded to a maximum quantum yield of photochemistry in PSII (F_v/F_m) of 0.7. The maximal growth rate for *Emiliana huxleyi* was 1.92 (d^{-1}), which corresponded to a maximum quantum yield of photochemistry in PSII (F_v/F_m) of 0.65. In Figure 8a and 7b, the relation between growth rate and variable fluorescence in *Thalassiosira pseudonana* and in *Emiliana huxleyi* is shown.

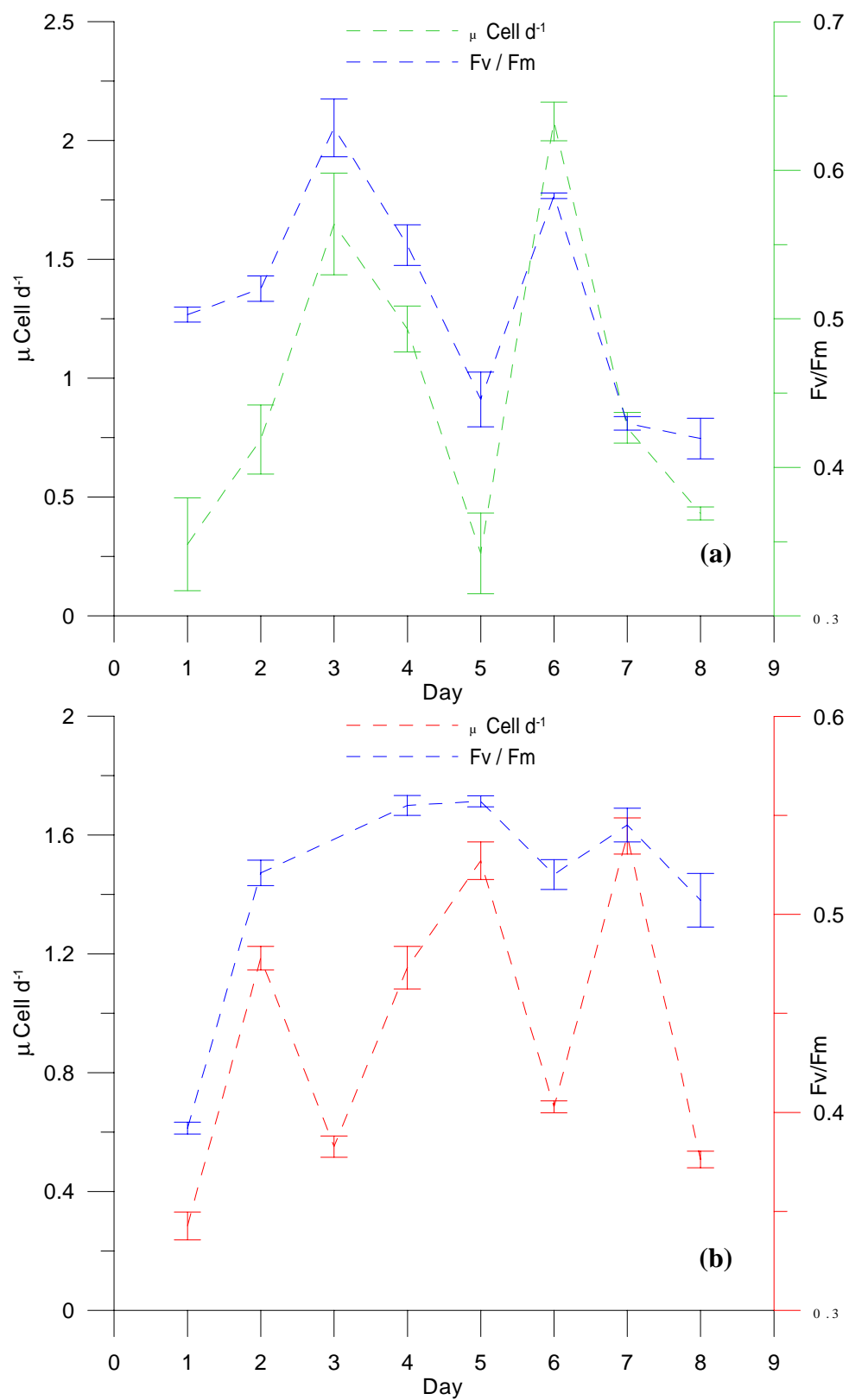


Figure 8. Growth rate and variable florescence for (a) *Thalassiosira pseudonana*; (b) *Emiliana huxleyi*

3.2 *Emiliana huxleyi* N and total C cell quotas

Samples for CHN analysis were collected during the two uptake experiments. The carbon results were for total coccolithophore carbon content, which includes cell carbon plus coccolith carbon. *Emiliana huxleyi* presented constant N cell quota of about 1.2 ± 0.04 pg cell⁻¹ and a ratio of total C to N of 11 (Figure 9).

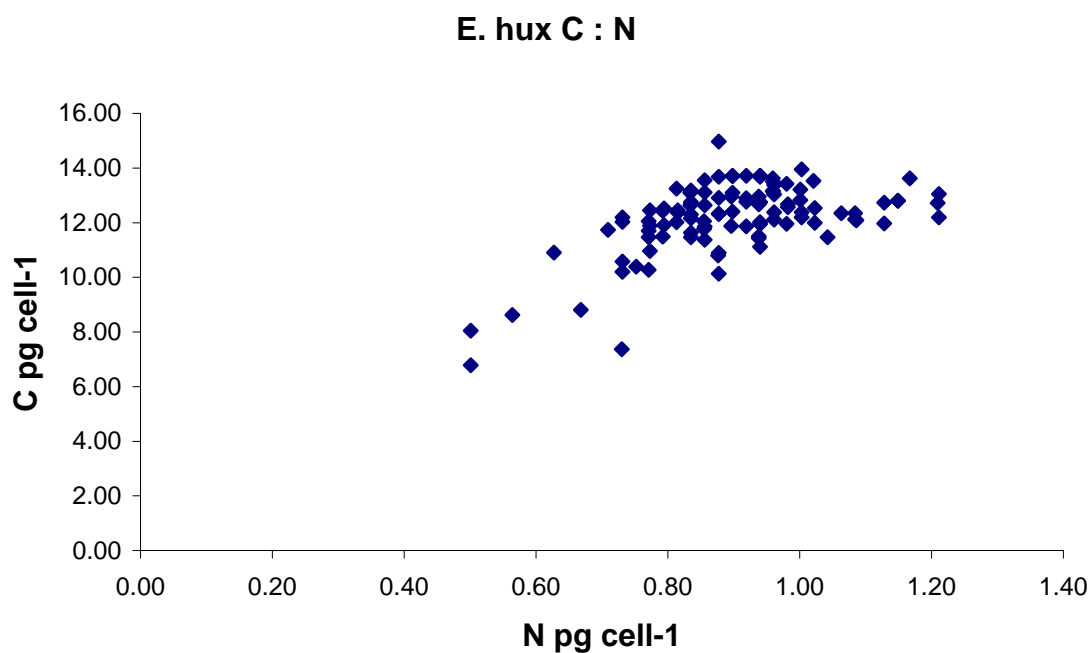


Figure 9. Total C:N in *Emiliana huxleyi* determined by CHN.

Samples were not collected for *Thalassiosira pseudonana*, because there is abundant information available in literature about this species C and N cell quotas.

3.3 *Emiliana huxleyi* nitrate uptake

The uptake experiment for *Emiliana huxleyi* was performed to obtain the nitrogen uptake rate for this organism given the lack of data in the literature. Data was noisy during the first half hour reflecting the low signal. The results for the 30-60 minutes interval gave uptake values ranged from 1.7 to $4.1 \cdot 10^{-9} \mu\text{M NO}_3 \text{ cell}^{-1} \text{ h}^{-1}$. With a Hanes-Wolfe plot not showed, it was possible to calculate a half saturation constant for *Emiliana huxleyi* of $0.3 \mu\text{mol N mL}^{-1}$.

3.4 Competition experiment

Three replicates of the competition experiments between *Emiliana huxleyi* and *Thalassiosira pseudonana* were performed and results were consistent between runs. In the first three days the diatom had higher growth rates and cell abundance than coccolithophores. Successively diatom growth rate and cell abundance was lower than the coccolithophore one, permitting a switch in dominance in the mix treatment (Figure 10). The switch in the phytoplankton dominance appeared due to the consumption of silicate in the first 2 days of the experiment treatment (Figure 11 b).

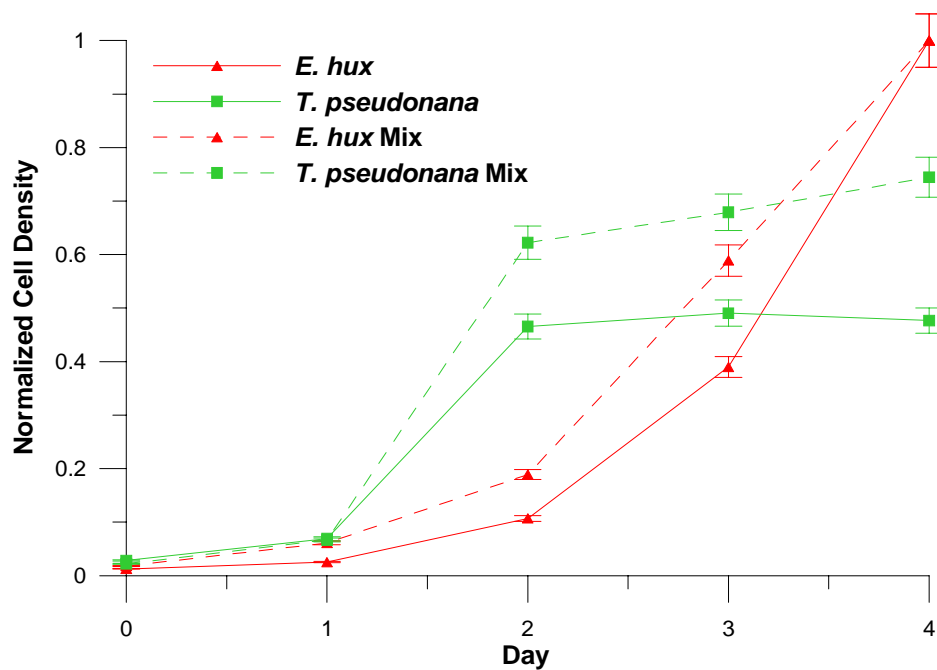


Figure 10. Normalized cell density in the three treatments of the competition experiment. *Emiliana huxleyi* (red solid line) in the control flask, (broken red line) in the mix batch; *Thalassiosira pseudonana* (green solid line) in the control flask, (broken green line) in the mix batch.

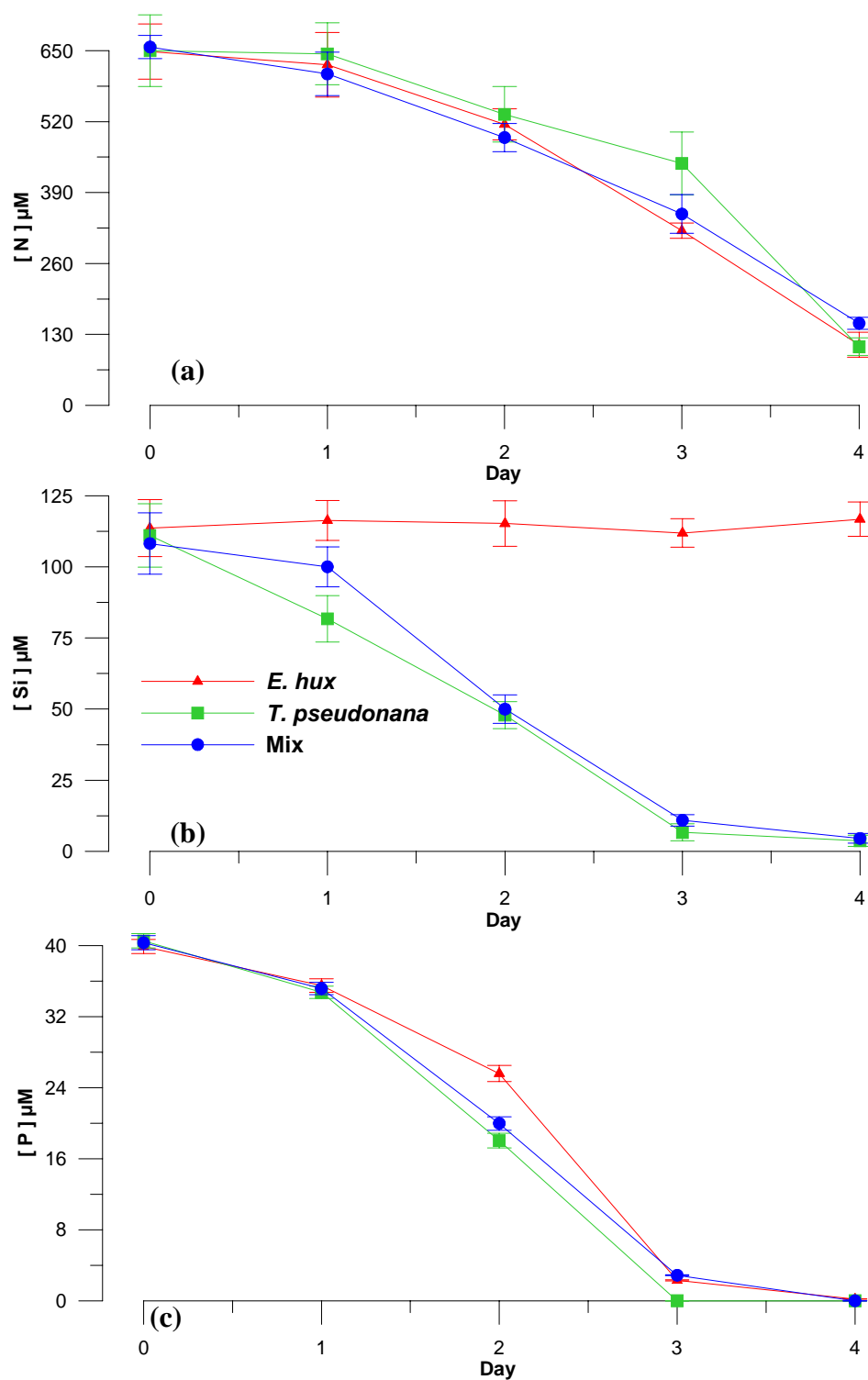


Figure 11. Time course of nutrients during the competition experiment in the three treatments. Monospecific batch culture of *Emiliana huxleyi* (red solid line); monospecific batch culture of *Thalassiosira pseudonana* (green solid line); mixed culture (blue broken line) (a) nitrate; (b) silicate; (c) phosphate.

3.5 Numerical simulation

A Monod model (eq. 1 and 2) and a mixed Droop-Monod model (eq. 6, 7 and 1, 2) were parameterized from literature and laboratory experimental results (Table 4, Table 5), for *Thalassiosira pseudonana* and *Emiliania huxleyi*. These models were used to test the effects of variable nutrient environments on coccolithophore and diatom performance, competition and succession. Both models produced reasonable estimates of growth rates and competition results.

Both models assume that the phytoplankton are limited by only one resource, nitrate. The resource is supplied as a series of pulses at intervals of 5, 13, 24, 120 hours to mimic respectively water-mixing due to internal waves, semidiurnal and diurnal tides, and average storm events in the ocean (Figure 12).

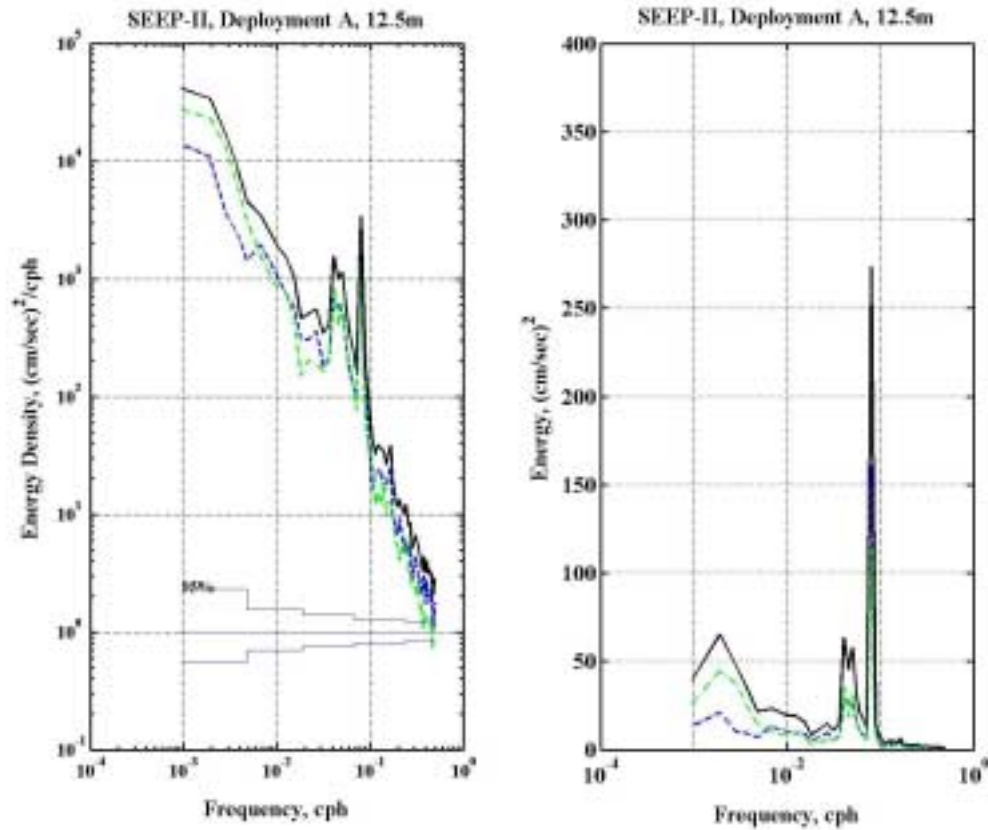


Figure 12. Power spectra of turbulence showing current data from ADCP from the Middle Atlantic Bight. Spectra were determined from 1048 hours long measurements with 50% overlaps. The first shows the spectra of the east and north components, plus the total spectrum, which is the sum of the spectra from the components, from 12.5 meters. (courtesy of Dr. C.N. Flagg)

3.5.1 Monod model

This model gives an immediate response of the cell growth rate to the external resource concentration but does not take into account intracellular nutrient storage. This model has been adopted to compare the uptake kinetics of diatoms and coccolithophores. With the given parameterization, and computing the equilibrium nutrient concentration for a specie grown alone at a given μ_{\max} (R^*) (Grover 1991), results that *Emiliania huxleyi* with an R^* of 1.26 is at a competitive disadvantage against *Thalassiosira pseudonana* which has an R^* of 1.4. The prediction given by the R^* changes if the system does not reach an equilibrium as in the case of a variable resource supply or batch mode.

Table 4. Parameters set for the Monod model

Parameter	Reference	
<i>Thalassiosira pseudonana</i>		
μ_{max} (h ⁻¹)	0.12	Present work
K _μ (μmol ml ⁻¹)	0.857	(Davidson and Gurney 1999)
Y (cells μmol ⁻¹)	5.9 x 10 ⁶	calculated from (Davidson and Gurney 1999)
<i>Emiliania huxleyi</i>		
μ_{max} (h ⁻¹)	0.08	Present work
K _μ (μmol ml ⁻¹)	0.3	(Tyrrell and Taylor 1995)
Y (cells μmol ⁻¹)	7.8 x 10 ⁶	calculated from (Muggli and Harrison 1996)
D (d ⁻¹)	0.07	

3.5.1.1 Competition in batch culture

The run of the model parameterized in Table 4 shows the dominance of *Thalassiosira pseudonana* over *Emiliania huxleyi*, in a batch system saturated with nutrients (Figure 13).

The outcome of this model is fully dependent on the maximal growth rate and the half saturation constant of the two organisms. Given the higher half saturation constant of the diatom, the only condition coccolithophores can dominate is in a starting nutrient concentration less than 1 μM NO_3 (Figure 14). This and the following run could be considered representative of a mid latitude summer condition with a stratified water column that has no nutrient input.

The higher affinity of the coccolithophore for nitrate allows it to outcompete the diatom in a low nutrient environment, as registered in the Sargasso Sea and vice versa in nutrient rich water as in the New York coastal waters diatom are the dominant with their fast uptake and higher half saturation constant (Hulburt 1970).

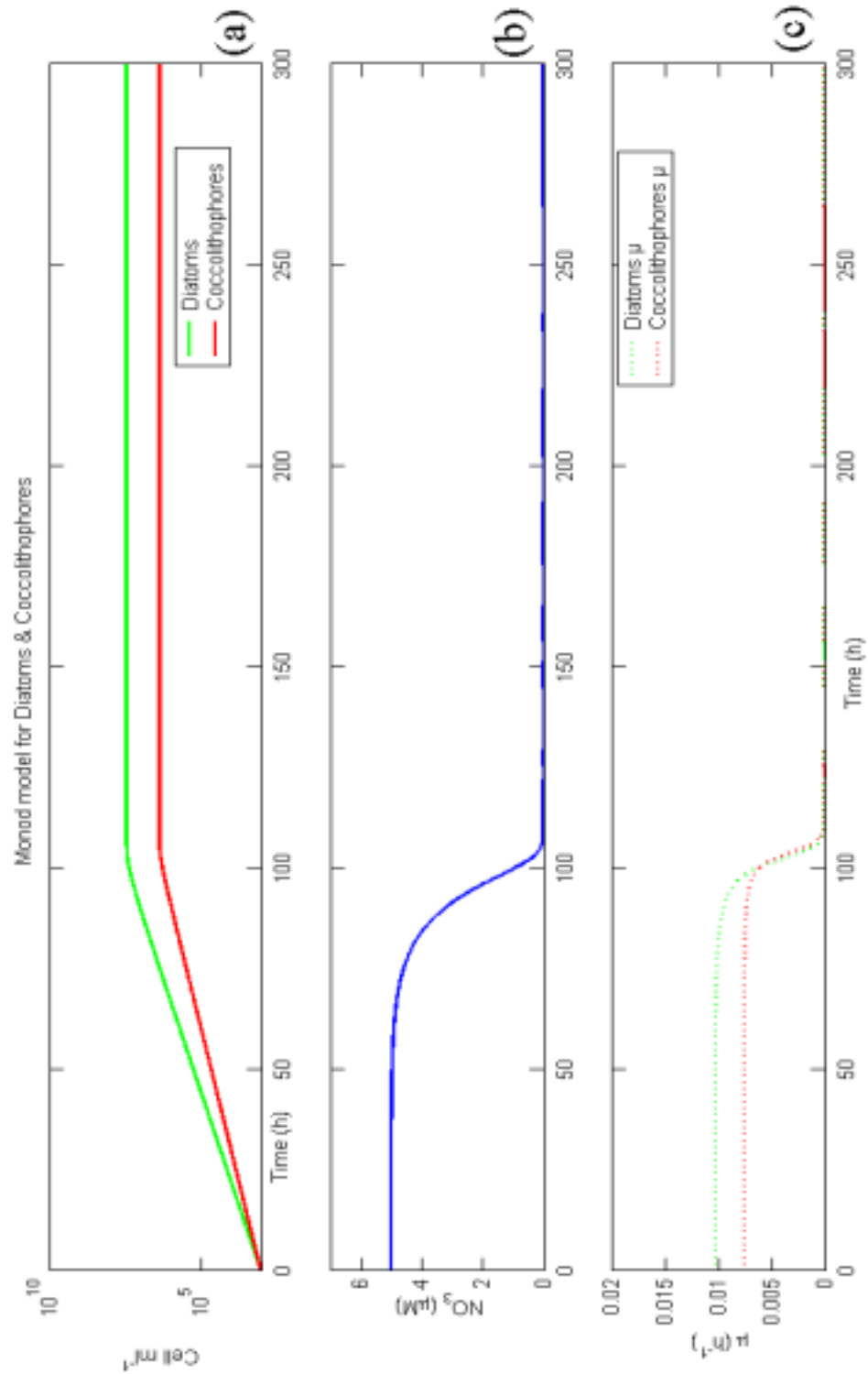


Figure 13. (a) Cell density of *Emiliania huxleyi* (red solid line) and *Thalassiosira pseudonana* (green solid line); (b) nutrient concentration in the system; (c) growth rate of *Emiliania huxleyi* (red dots) and *Thalassiosira pseudonana* (green dots) according to the Monod model without cell death or wash-out and with a starting NO₃ concentration of 5 μM.

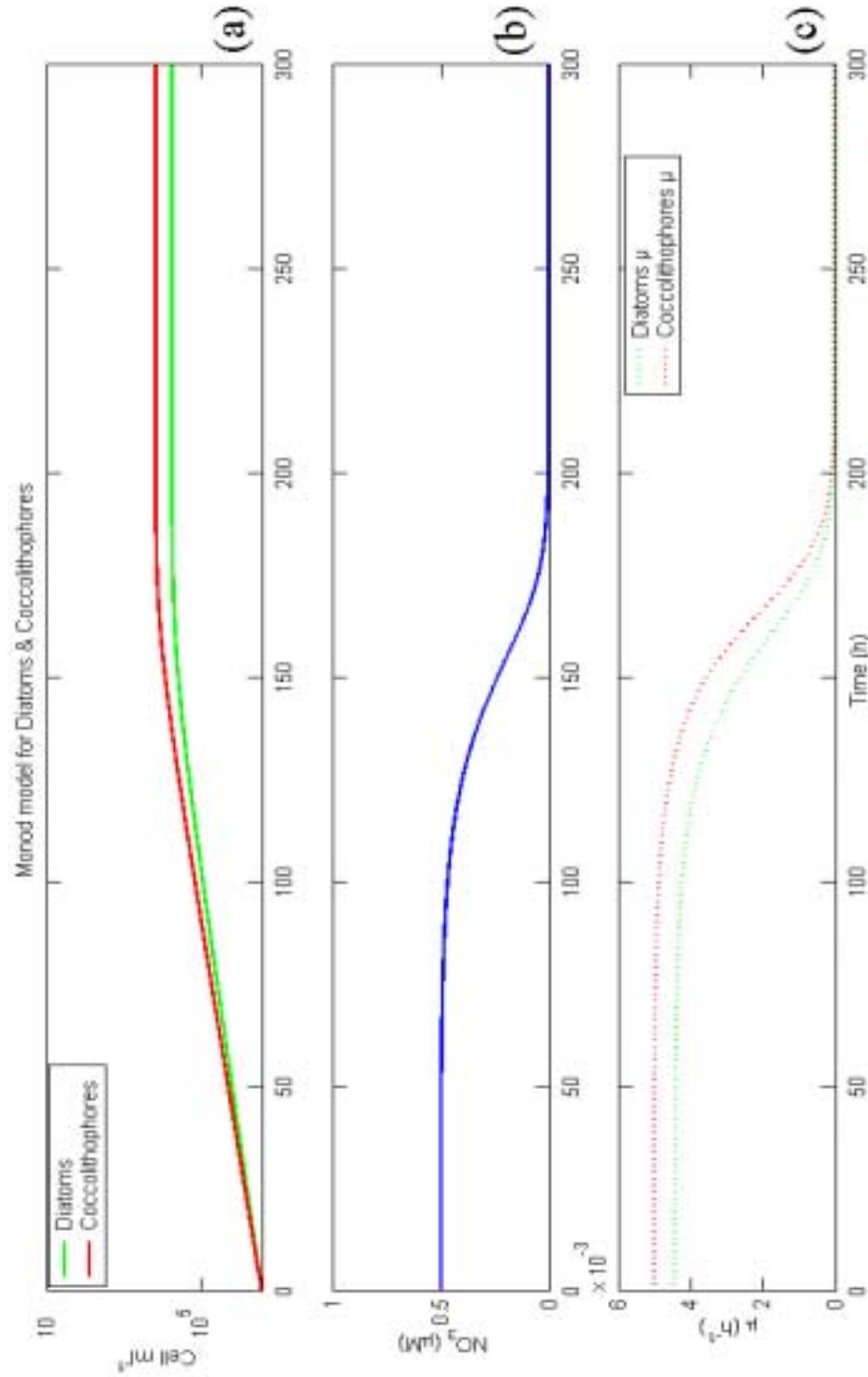


Figure 14. (a) Cell density of *Emiliania huxleyi* (red solid line) and *Thalassiosira pseudonana* (green solid line); (b) nutrient concentration in the system; (c) growth rate of *Emiliania huxleyi* (red dots) and *Thalassiosira pseudonana* (green dots) according to the Monod model without cell death or wash-out and with a starting NO₃ concentration of 5 μM.

3.5.1.2 Competition in continuous resource supply

By adding a component to the model that considers washout or death of the cells, it is possible to obtain a constant nutrient concentration in the system. If this is above the critical value of $0.8 \mu\text{M}$, then the diatom will always dominate and the coccolithophore will eventually be washed out of the system (Figure 15), vice versa if the nutrient concentration is maintained at $0.8 \mu\text{M}$ or lower (Figure 16).

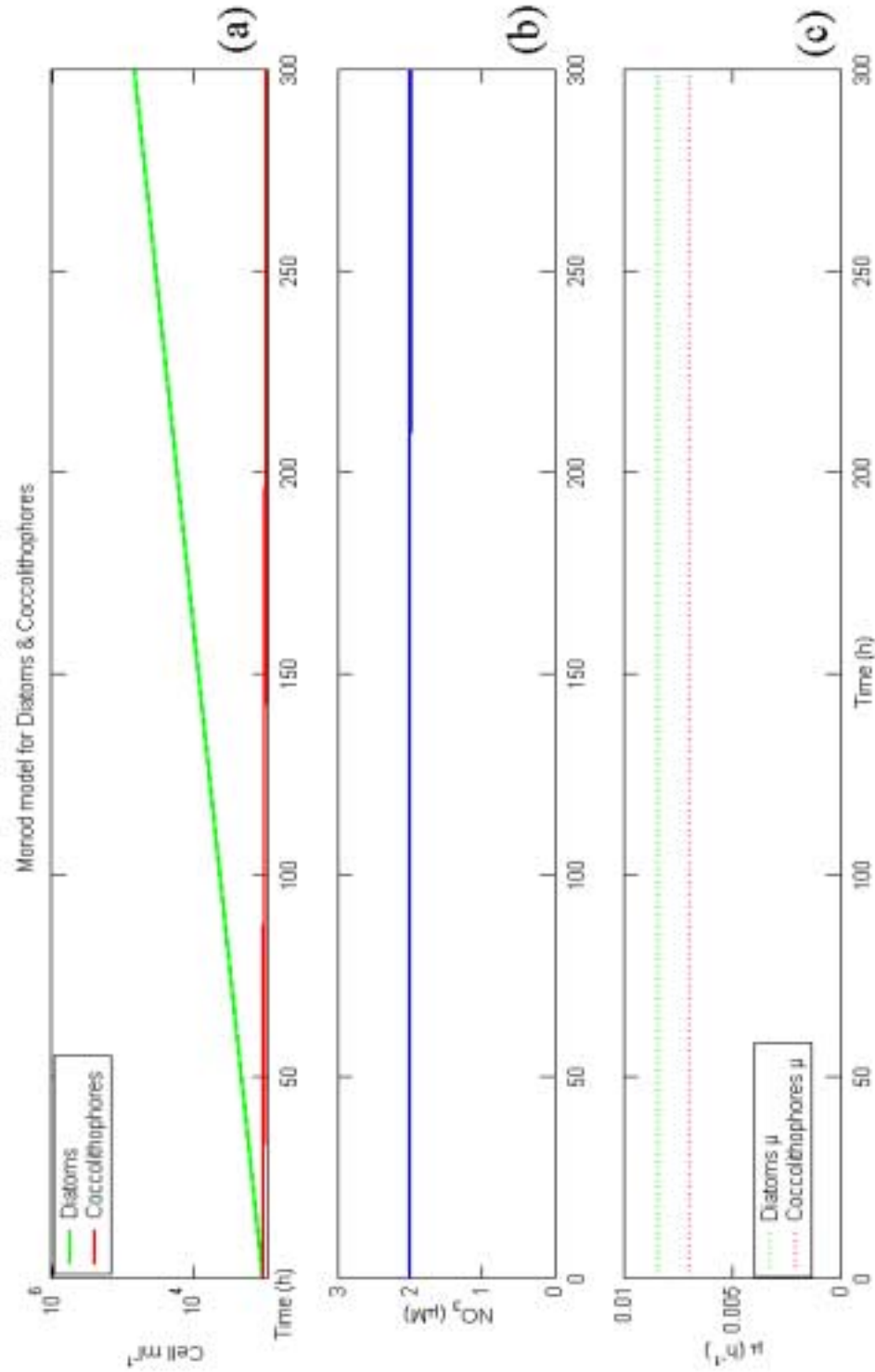


Figure 15. (a) Cell density of *Emiliania huxleyi* (red solid line) and *Thalassiosira pseudonana* (green solid line); (b) NO₃ concentration in the system; (c) growth rate of *Emiliania huxleyi* (red dots) and *Thalassiosira pseudonana* (green dots) according to the Monod model (eq. 1) with a starting NO₃ concentration of 2 μM and a constant input of 2 μM.

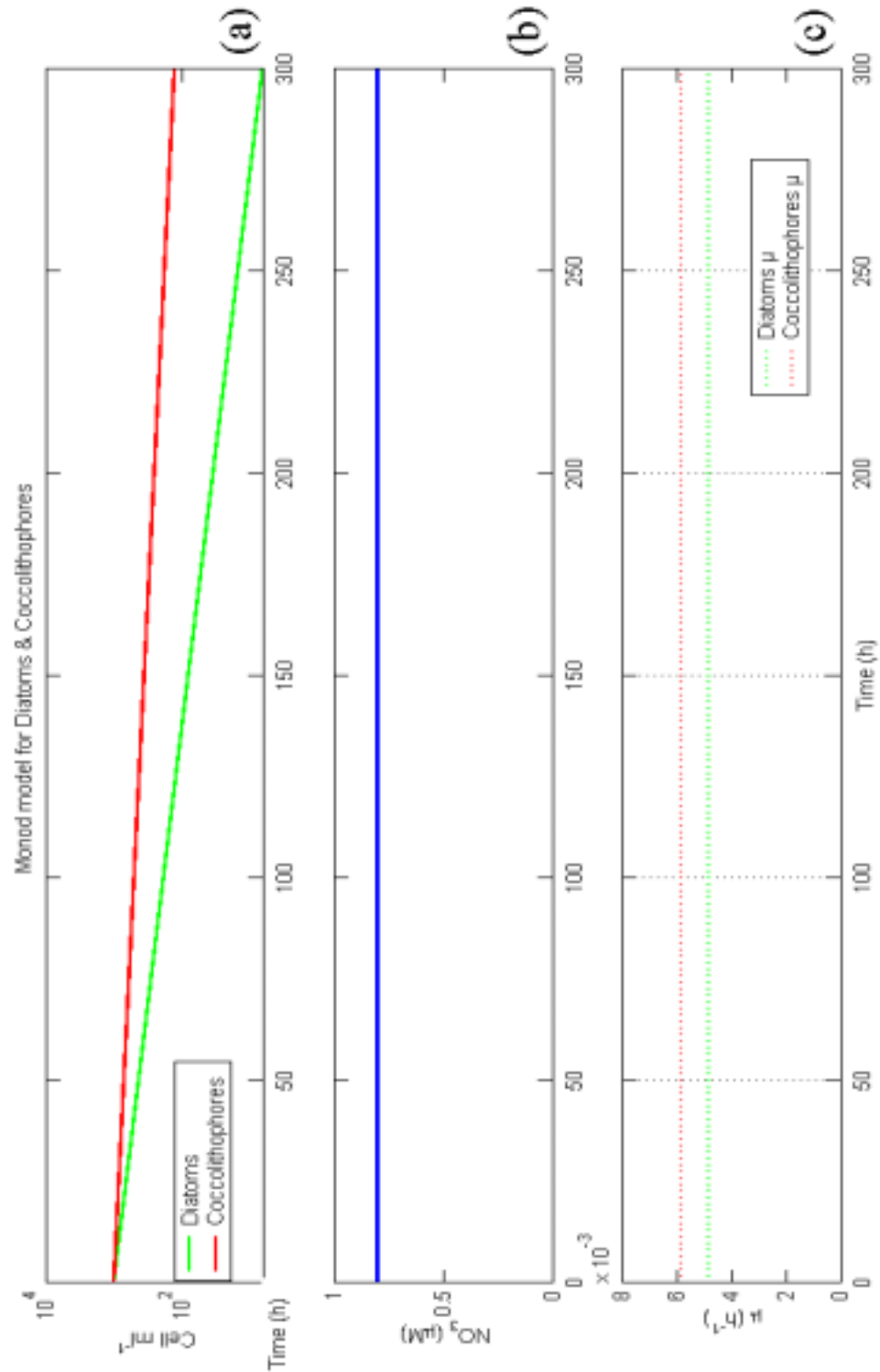


Figure 16. (a) Cell density of *Emiliania huxleyi* (red solid line) and *Thalassiosira pseudonana* (green solid line); (b) NO₃ concentration in the system; (c) growth rate of *Emiliania huxleyi* (red dots) and *Thalassiosira pseudonana* (green dots) according to the Monod model (eq. 1) with a starting NO₃ concentration of 0.8 μM, a constant input of 0.8 μMh⁻¹, and a dilution rate of 0.7.

3.5.1.3 Competition with a pulsed resource supply

For competition in pulsed nutrient regimes, the set of ordinary differential equation could not be solved for pulses with lengths smaller than 15-30% of the pulse period, due to the stiffness of the problem. Stiffness occurs when there are two or more very different scales for the independent variable from which the dependent variables are changing. The diatoms outcompeted the coccolithophores in the 5, 13, 24 hours pulse run, but the coccolithophores completely dominated in the 120 hours pulse run. These runs were made with a low background concentration of nitrate; the pulse of 3 μ moles was distributed on the minimal length required for the model to resolve all the pulses over a 1000 hours. The growth rate of diatoms is higher, than the dilution rate only in the 5 hours pulse run. In all others runs, both organisms were persistent for the 1000 hours of the run but tended to be both washed-out.

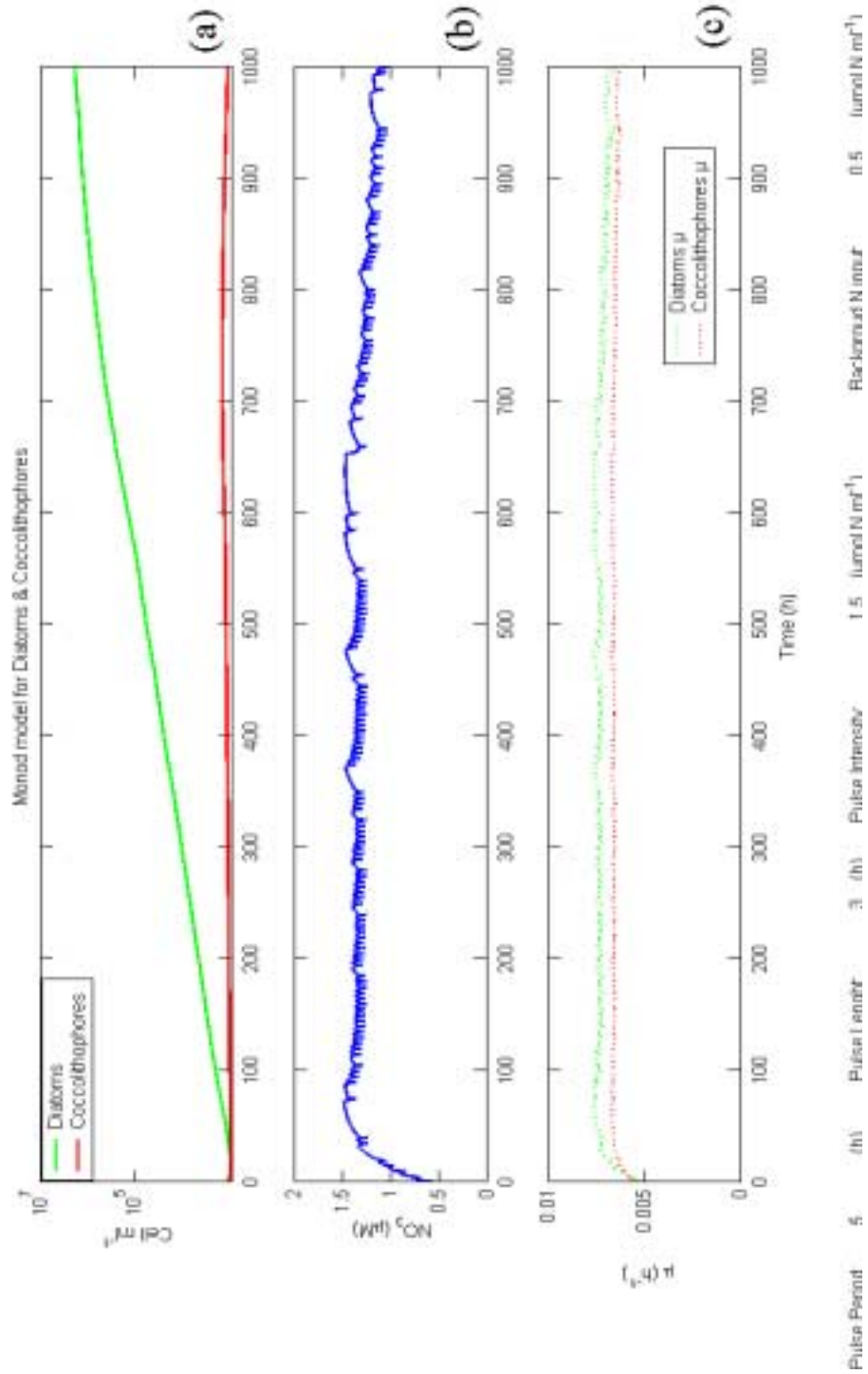


Figure 17. (a) Cell density of *Emiliania huxleyi* (red solid line) and *Thalassiosira pseudonana* (green solid line); (b) NO_3 concentration in the system; (c) growth rate of *Emiliania huxleyi* (red dots) and *Thalassiosira pseudonana* (green dots) according to the Monod model (eq. 1) with a starting NO_3 concentration of $0.5 \mu\text{M}$, a background input of $0.5 \mu\text{Mh}^{-1}$ and a dilution rate of 0.7 , a pulse period of 5 hours and a pulse length of 3 hours.

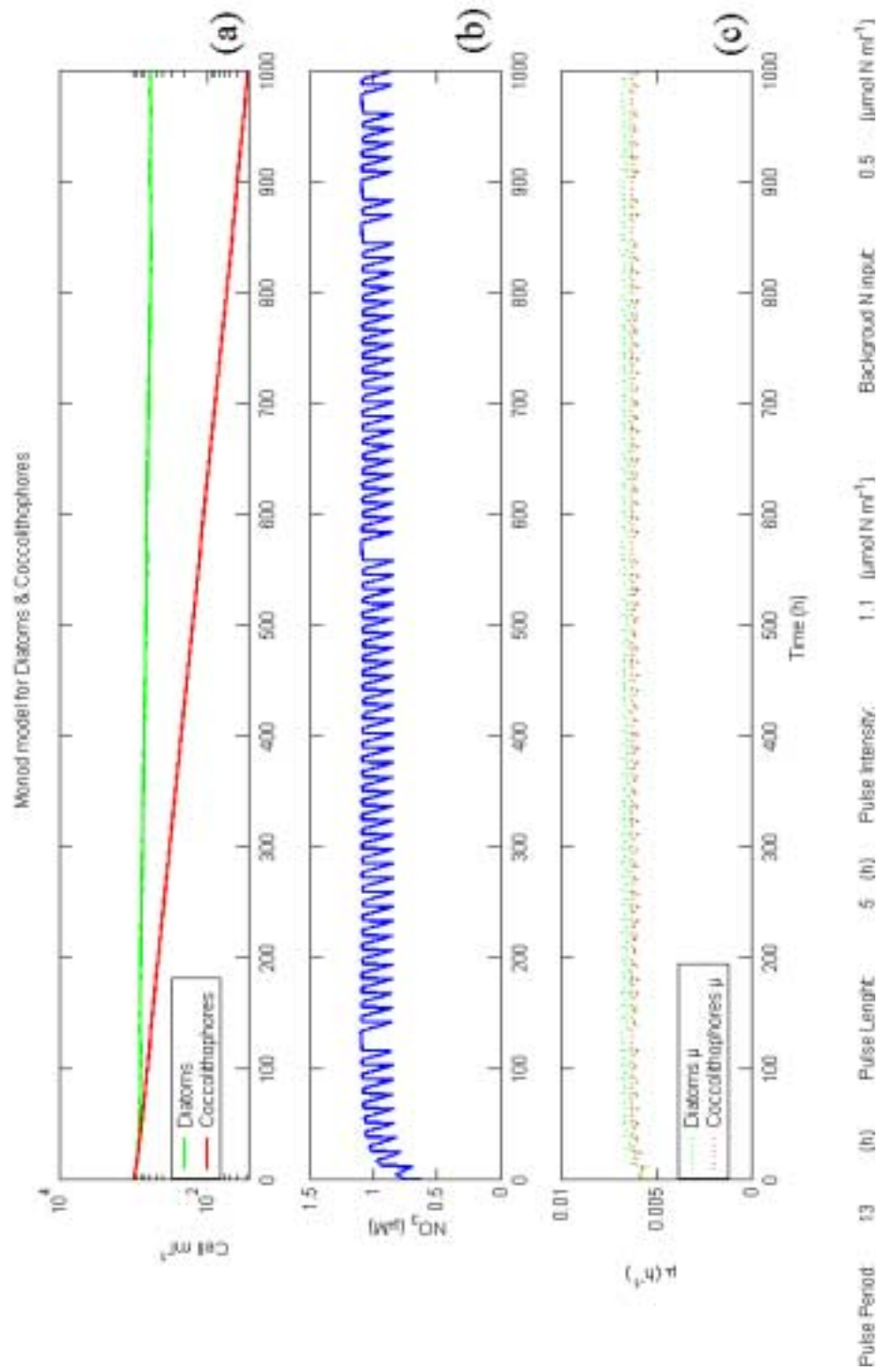


Figure 18. (a) Cell density of *Emiliania huxleyi* (red solid line) and *Thalassiosira pseudonana* (green solid line); (b) NO₃ concentration in the system; (c) growth rate of *Emiliania huxleyi* (red dots) and *Thalassiosira pseudonana* (green dots) according to the Monod model (eq. 1) with a starting NO₃ concentration of 0.5 μM, a background input of 0.5 μMh⁻¹ and a dilution rate of 0.7, a pulse period of 13 hours and a pulse length of 5 hours.

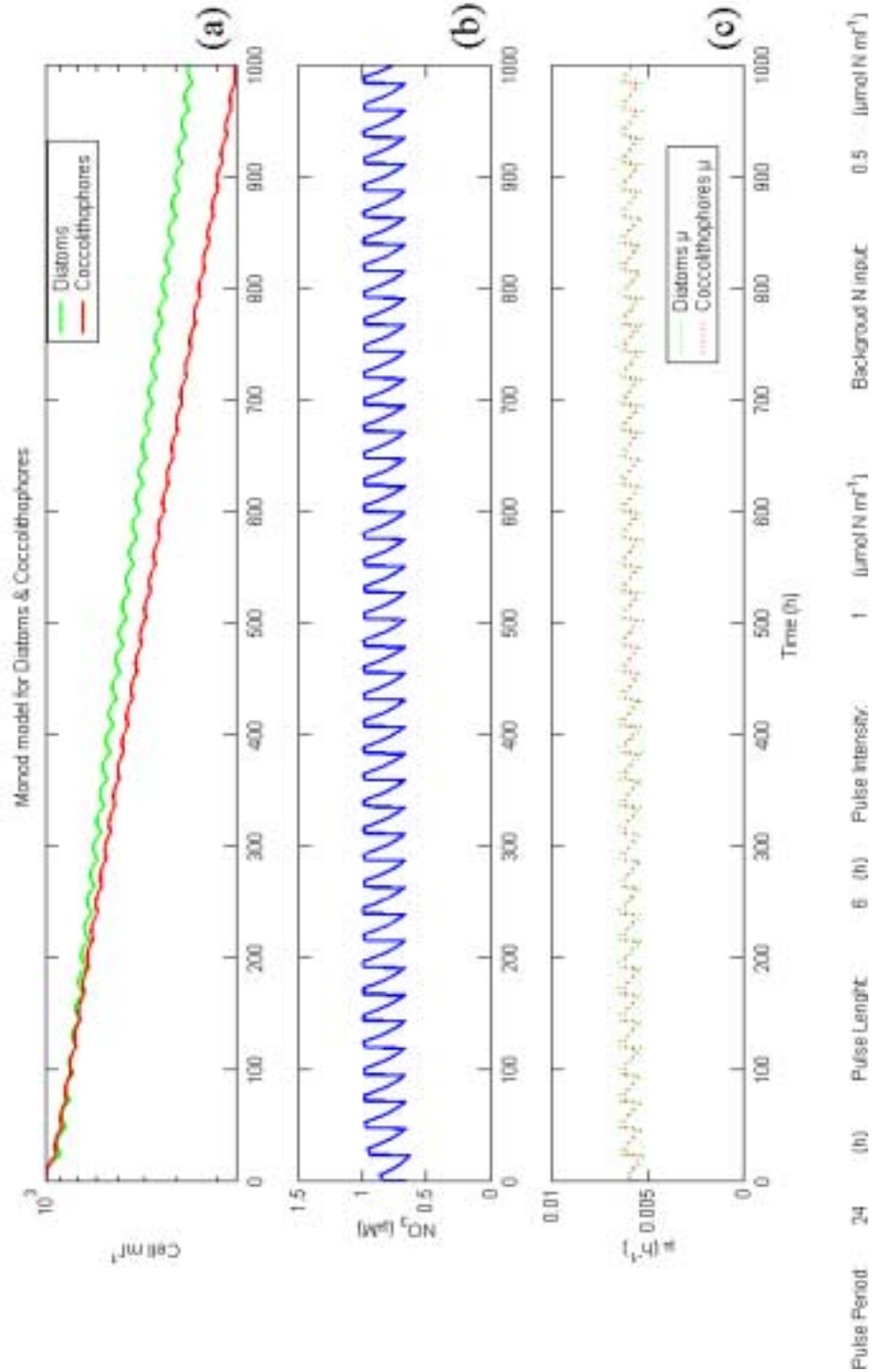


Figure 19. (a) Cell density of *Emiliania huxleyi* (red solid line) and *Thalassiosira pseudonana* (green solid line); (b) NO₃ concentration in the system; (c) growth rate of *Emiliania huxleyi* (red dots) and *Thalassiosira pseudonana* (green dots) according to the Monod model (eq. 1) with a starting NO₃ concentration of 0.5 μM, a constant input of 0.5 μMh⁻¹ and a dilution rate of 0.7, a pulse period of 24 hours and a pulse length of 6 hours.

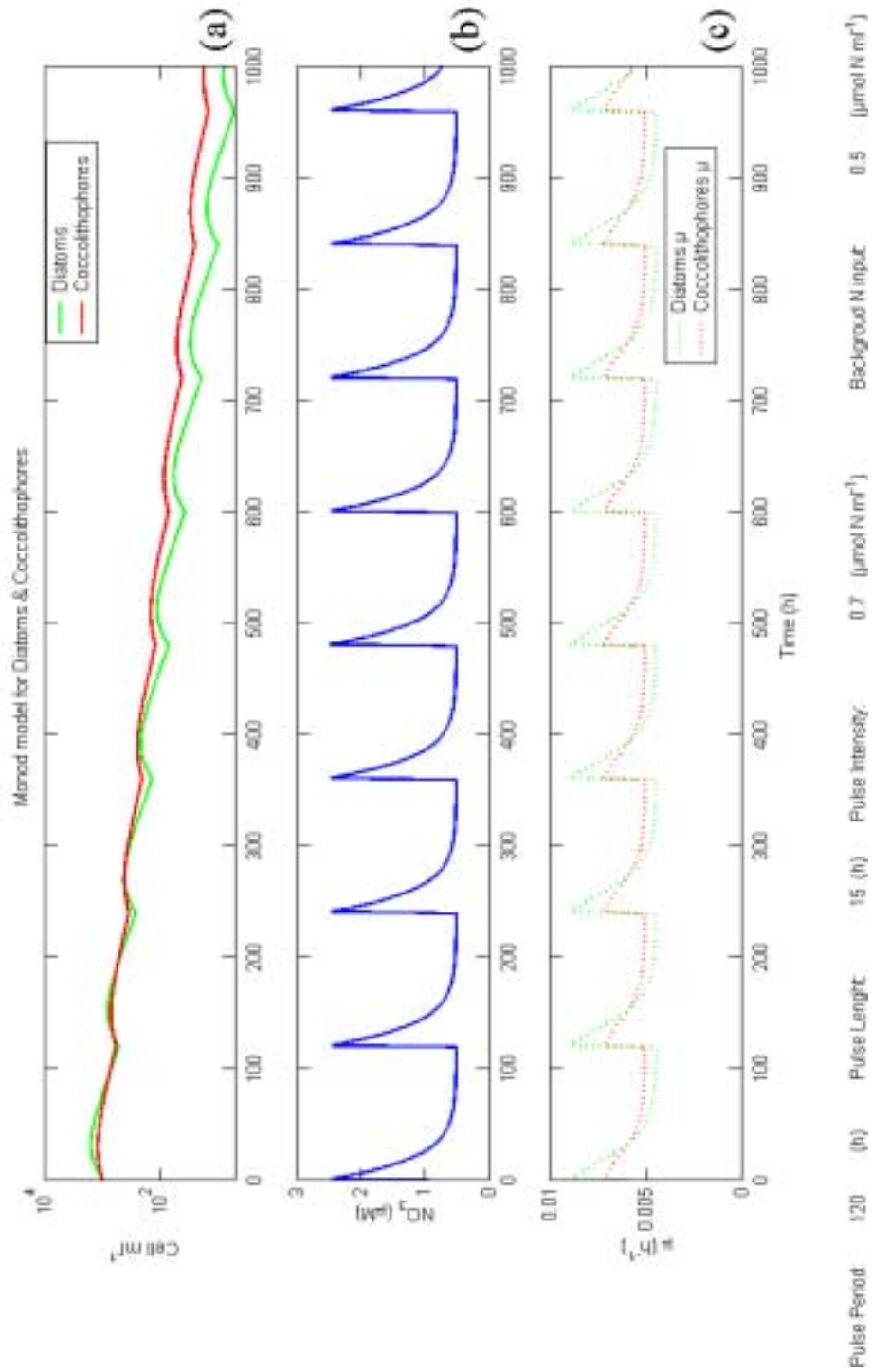


Figure 20. (a) cell density of *Emiliania huxleyi* (red solid line) and *Thalassiosira pseudonana* (green solid line); (b) NO₃ concentration in the system; (c) growth rate of *Emiliania huxleyi* (red dots) and *Thalassiosira pseudonana* (green dots) according to the Monod model (eq. 1) with a starting NO₃ concentration of 0.5 μM, a background input of 0.5 μMh⁻¹ and a dilution rate of 0.7, a pulse period of 120 hours and a pulse length of 15 hours.

These results suggest that differences in the physiology of diatoms and coccolithophores give them an advantage in different nutrient pulse regimes. The diatoms are always dominant in more turbulent environments. Water masses with higher mixing rates have higher nutrient concentration than the more stable environment, where coccolithophores are able to outcompete the diatoms.

3.5.2 Mixed Droop-Monod model

To test the second hypothesis, which is the advantage of diatoms over the coccolithophores in a pulsed regime, due to vacuole storage capacity, a mixed Droop-Monod model was used. With these runs, I tested when and what type of nutrient pulse is advantageous for the diatoms. This effect was simulated considering the growth rate function, not only of the substrate concentration, but also of the N cell quota as presented in equation 3.

Table 5. Parameters set for the Mixed Droop-Monod model

Parameter		
<i>Diatom</i>		
μ_{\max} (h ⁻¹)	0.12	Present work
K_p (μmol L ⁻¹)	0.857	(Davidson and Gurney 1999)
Q_{\min} (μmol cell ⁻¹)	5.0×10^{-8}	(Davidson and Gurney 1999)
Q_{\max} (μmol cell ⁻¹)	2.8×10^{-7}	(Davidson and Gurney 1999)
ρ_{\max} (μmol cell ⁻¹ h ⁻¹)	1.7×10^{-8}	(Davidson and Gurney 1999)
<i>Coccolithophore</i>		
μ_{\max} (h ⁻¹)	0.08	Present work
K_{μ} (μmol ml ⁻¹)	0.3	(Tyrrell and Taylor 1995)
Y (cells μmol ⁻¹)	7.7×10^6	calculated from (Muggli and Harrison 1996)

3.5.1.3 Competition in batch culture

In the case of the mixed Droop-Monod model, the diatom growth rate is slightly lowered in nutrient replete conditions, but confers an advantage between hours 140 and 160 (Figure 21). This reflects the storage capacity of the vacuole and allows the diatoms to maintain a higher growth rate even when the nutrient concentration is close to zero. Figure 21 shows the output for a batch mode condition without the addition of nutrients and washout of cells. A stratified water column is simulated here with an absence of mixing that brings nutrient and washes out cells.

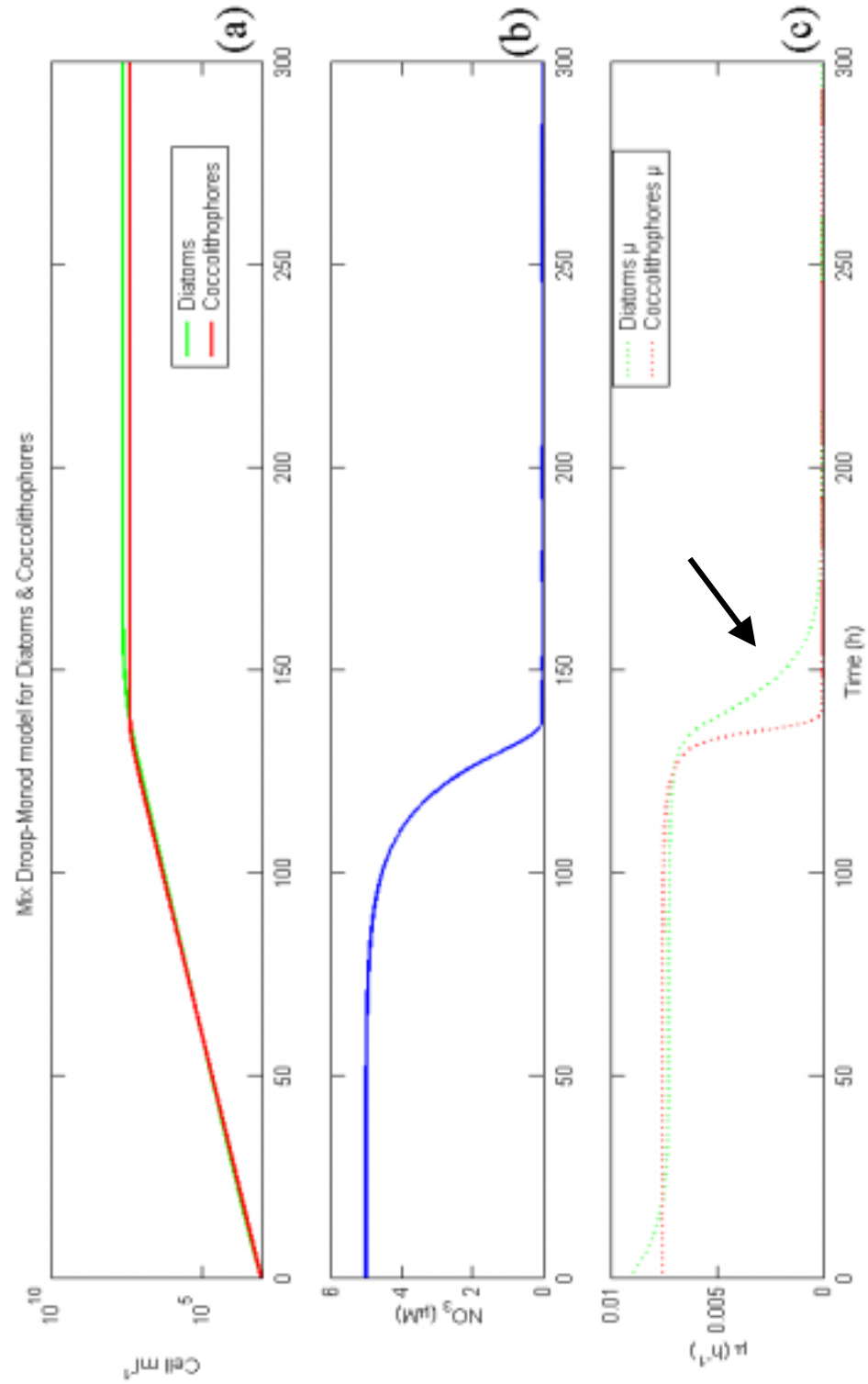


Figure 21. (a) cell density of *Emiliania huxleyi* (red solid line) and *Thalassiosira pseudonana* (green solid line); (b) nutrient concentration in the system; (c) growth rate of *Emiliania huxleyi* (red dots) and *Thalassiosira pseudonana* (green dots) according to the Mixed Droop-Monod model without cell death or wash-out and with a starting NO₃ concentration of 5 μM.

3.5.1.4 Competition in continuous resource supply

In the case of the continuously mixed Droop-Monod model, the critical NO_3 concentration at which it is possible to see a switch in dominance is $2 \mu\text{M}$. As shown in Figure 22, starting with a concentration of $2 \mu\text{M}$ NO_3 and adding the same concentration, the model indicates a switch of dominance from diatoms to coccolithophores at about 90.

3.5.1.5 Competition with pulsed resource supply

Diatoms clearly have an advantage in an environment in which nutrients are pulsed with high frequency, 5, 13, 24 hours (Figure 23, Figure 24, Figure 25). However at 120 hours period pulse (Figure 26), coccolithophores outcompete the diatoms.

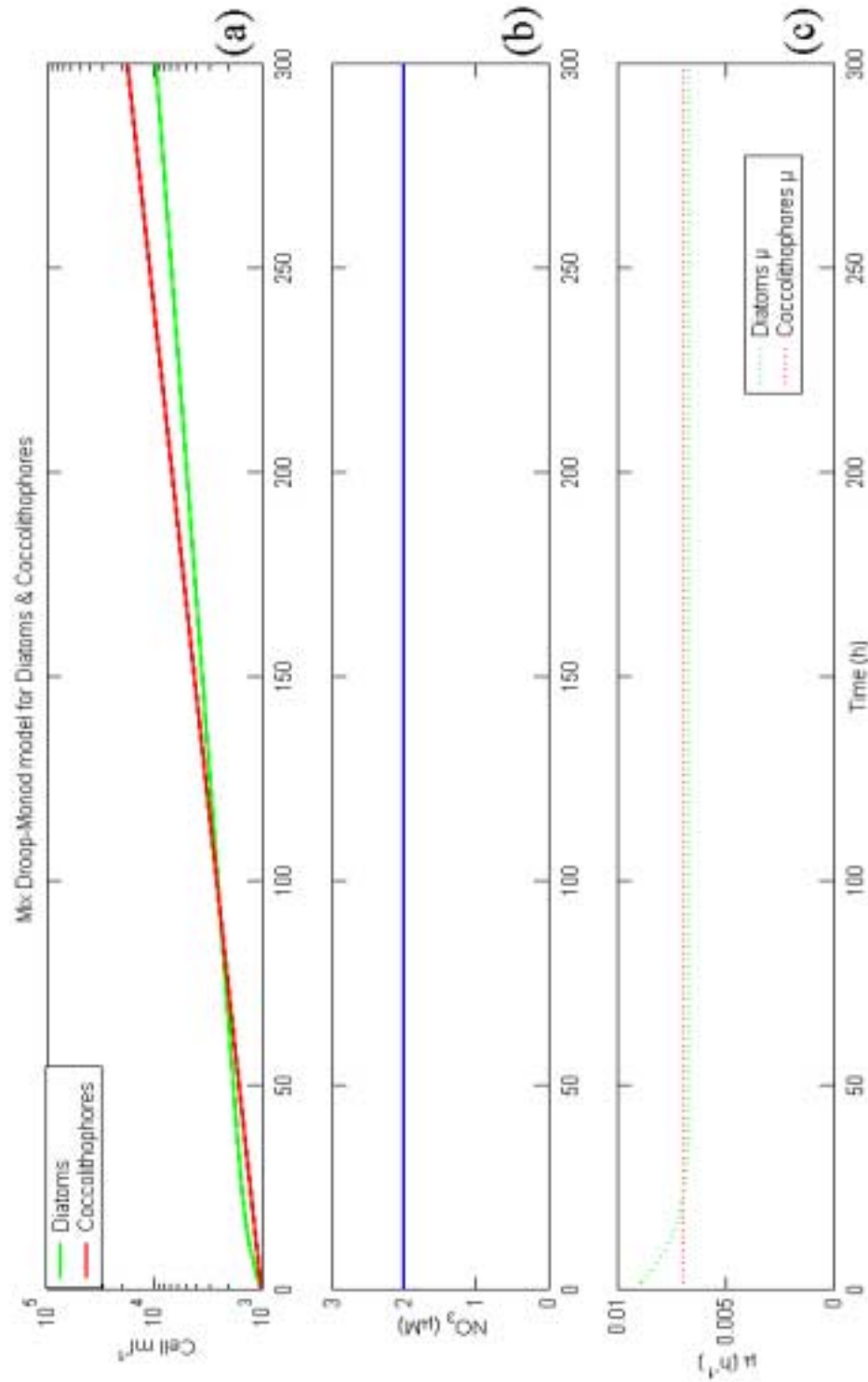


Figure 22. (a) cell density of *Emiliania huxleyi* (red solid line) and *Thalassiosira pseudonana* (green solid line); (b) nutrient concentration in the system; (c) growth rate of *Emiliania huxleyi* (red dots) and *Thalassiosira pseudonana* (green dots) according to the Mix Droop-Monod model with a starting NO_3 concentration of $2 \mu\text{M}$, a constant input of $2 \mu\text{M h}^{-1}$, and dilution rate of 0.7.

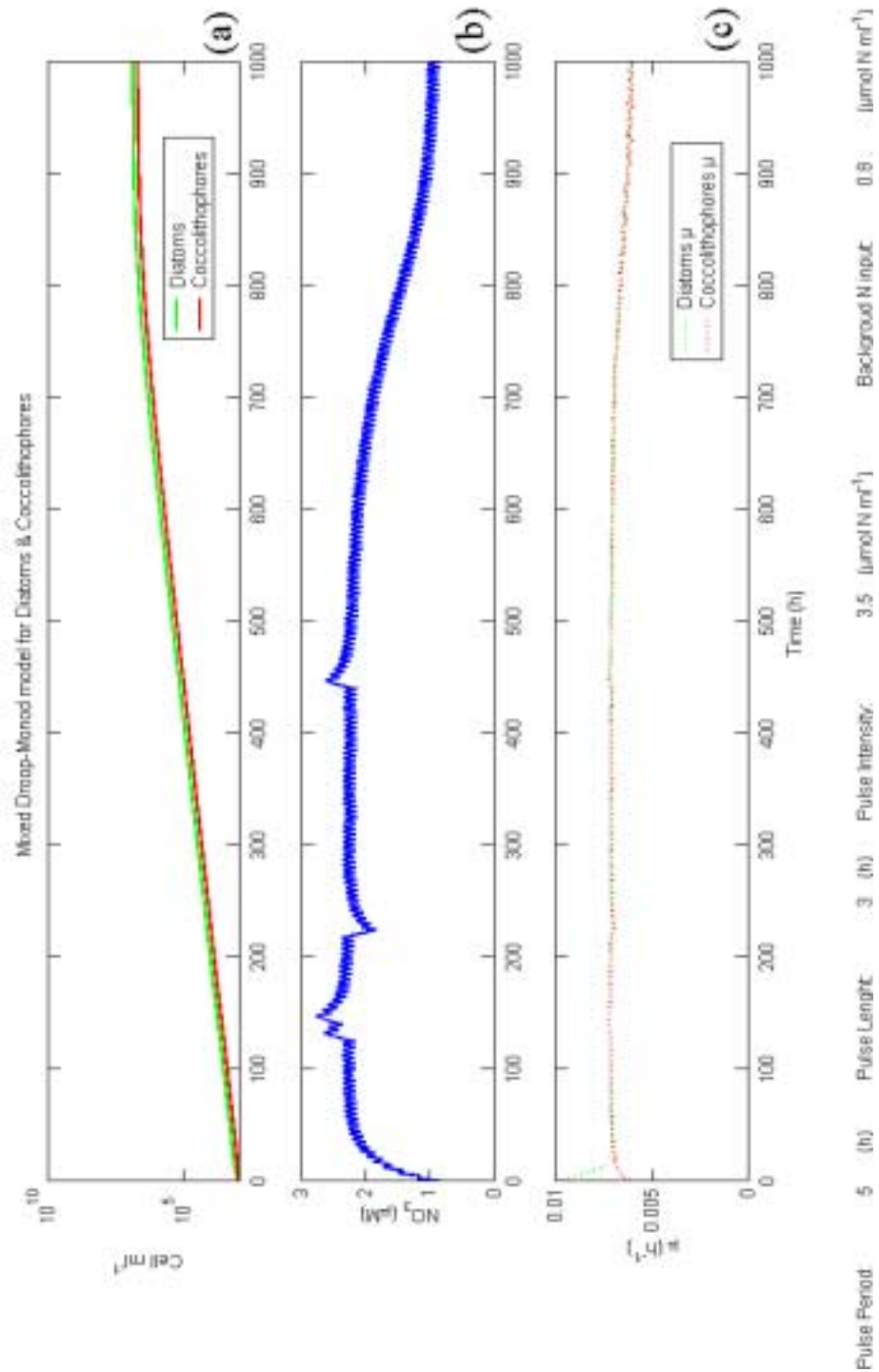


Figure 23. (a) Cell density of *Emiliania huxleyi* (red solid line) and *Thalassiosira pseudonana* (green solid line); (b) nutrient concentration in the system; (c) growth rate of *Emiliania huxleyi* (red dots) and *Thalassiosira pseudonana* (green dots) according to the Mixed Droop-Monod model) with a starting NO₃ concentration of 0.8 μM, a background input of 0.8 μMh⁻¹ and a dilution rate of 0.6, a pulse period of 5 hours and a pulse length of 3 hours.

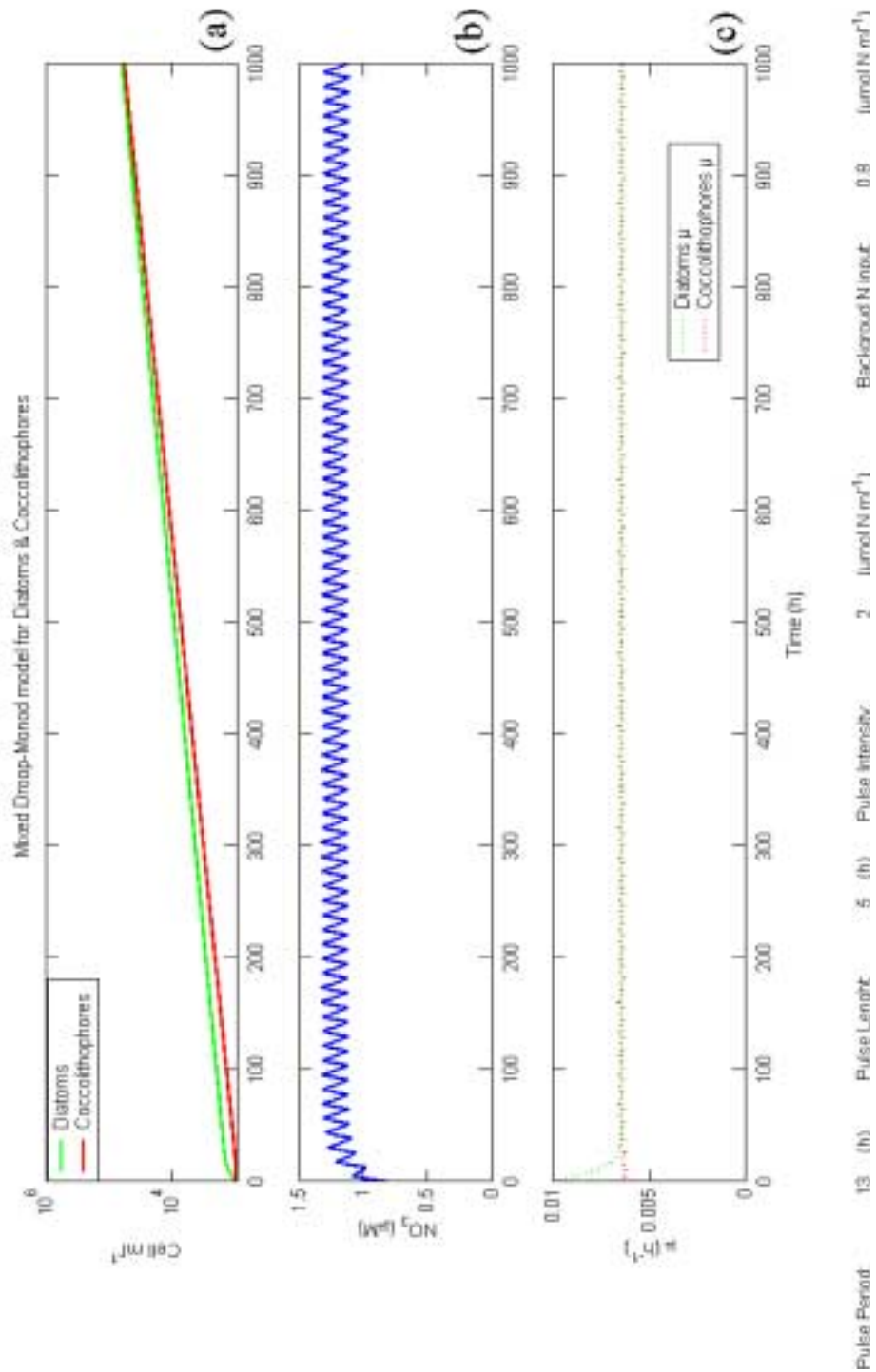


Figure 24. (a) Cell density of *Emiliania huxleyi* (red solid line) and *Thalassiosira pseudonana* (green solid line); (b) nutrient concentration in the system; (c) growth rate of *Emiliania huxleyi* (red dots) and *Thalassiosira pseudonana* (green dots) according to the Mixed Droop-Monod model) with a starting NO₃ concentration of 0.8 μM, a background input of 0.8 μMh⁻¹ and a dilution rate of 0.6, a pulse period of 13 hours and a pulse length of 5 hours.

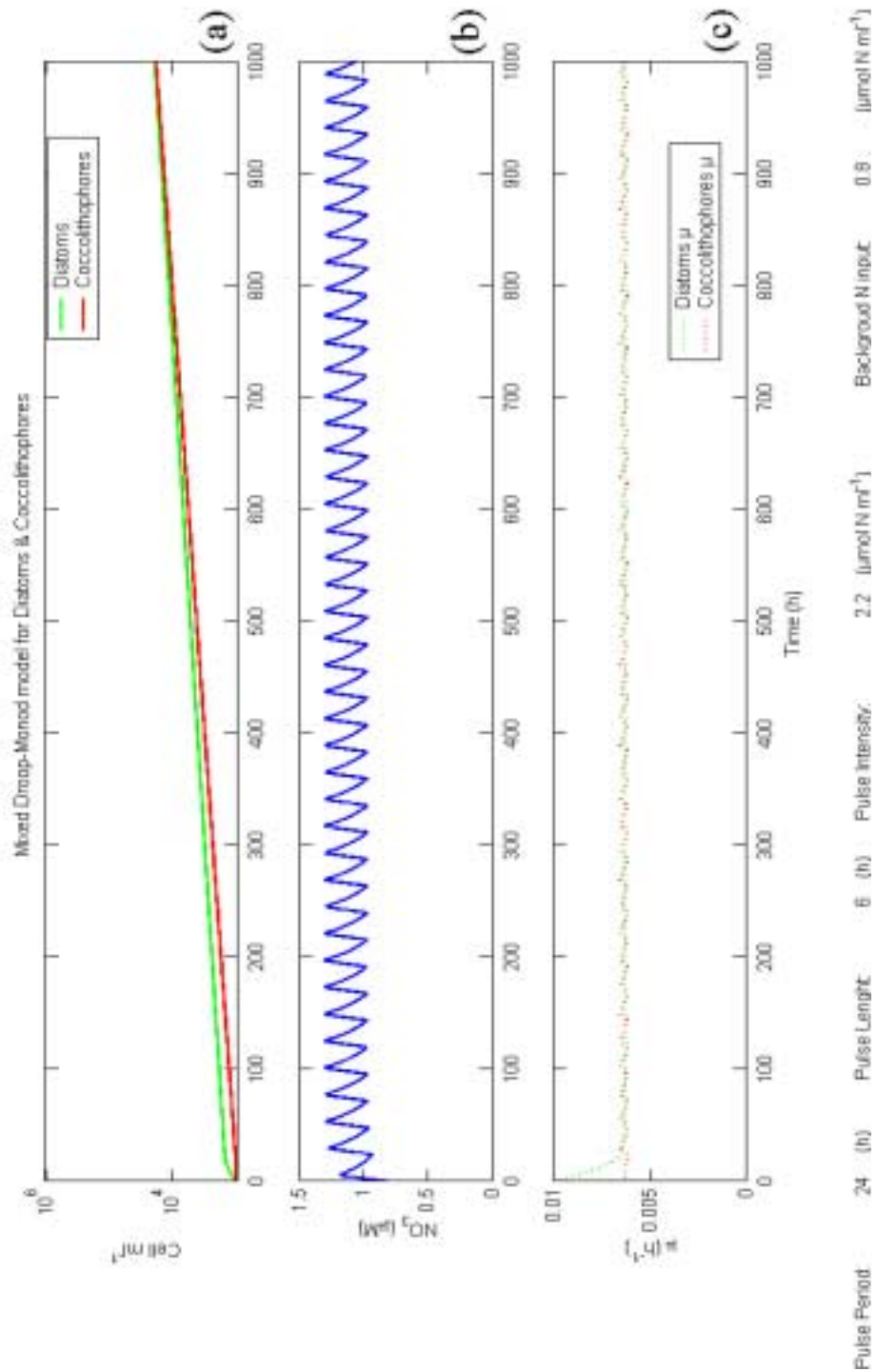


Figure 25. (a) Cell density of *Emiliania huxleyi* (red solid line) and *Thalassiosira pseudonana* (green solid line); (b) nutrient concentration in the system; (c) growth rate of *Emiliania huxleyi* (red dots) and *Thalassiosira pseudonana* (green dots) according to the Mixed Droop-Monod model) with a starting NO₃ concentration of 0.8 μM, a background input of 0.5 μMh⁻¹ and a dilution rate of 0.8, a pulse period of 24 hours and a pulse length of 6 hours.

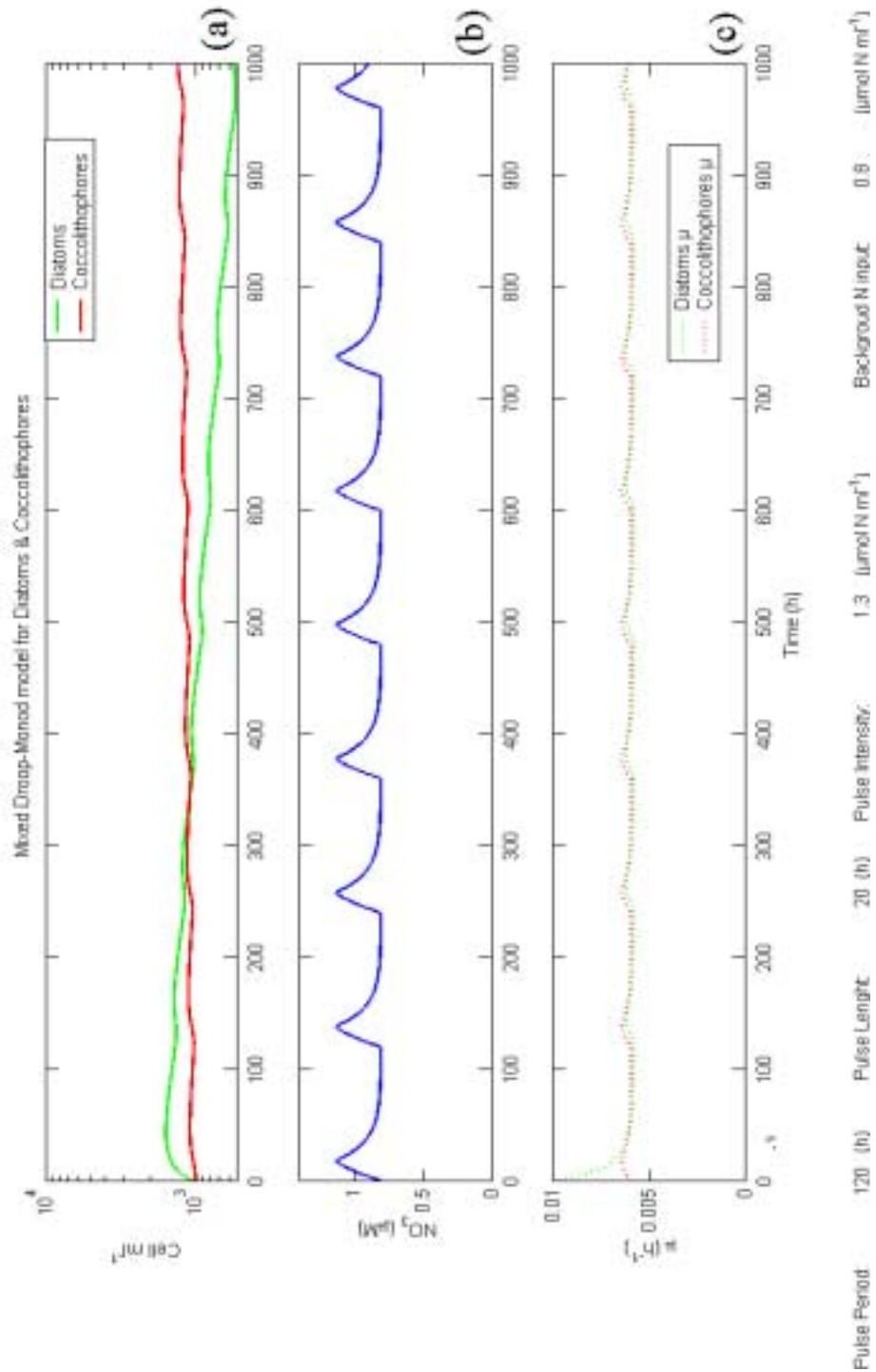


Figure 26. (a) Cell density of *Emiliania huxleyi* (red solid line) and *Thalassiosira pseudonana* (green solid line); (b) nutrient concentration in the system; (c) growth rate of *Emiliania huxleyi* (red dots) and *Thalassiosira pseudonana* (green dots) according to the Mixed Droop-Monod model) with a starting NO₃ concentration of 0.8 μM, a background input of 0.8 μMh⁻¹ and a dilution rate of 0.6, a pulse period of 120 hours and a pulse length of 20 hours.

4 Discussion

The laboratory experiments represent significant preliminary results. All the instrumental techniques produced consistent data, that is, Chl *a*, CHN, coulter counter and nutrient analyses gave numbers that reflect those previously found in the literature for both organisms. The growth rates were also consistent with those one found in the literature for similar experimental setups. A good agreement was found between the growth rate and Fv/Fm corroborating the relationship between the cells' phytophysiological efficiency and growth rate.

The N cell quota of *Emiliana huxleyi* appeared constant and independent of the nutrient treatment, supporting the use of the Monod model to simulate the physiology of this organism. Future C and N cell quota experiments on coccolithophores will utilize bigger filters, which will consent sub-samples to be measured for both total and organic carbon, to verify the grade of calcification of the cells.

The results of the NO₃ uptake experiment, $1.7 \text{ to } 4.1 \cdot 10^{-9} \mu\text{M NO}_3 \text{ cell}^{-1} \text{ h}^{-1}$, were in the range of the uptake calculated by the growth rate times the cell quota, $1.2 \text{ to } 7.6 \cdot 10^{-9} \mu\text{M NO}_3 \text{ cell}^{-1} \text{ h}^{-1}$ [Muggli, 1996 #536; Muggli, 1997 #597; Fernández, 1996 #663].

With the batch culture competition experiment, competitive dominance of diatoms to coccolithophores was dependant on nutrient concentration. This experiment simulated a stratified water column, typical of summer conditions at temperate latitudes. The diatoms initially grew faster than the coccolithophores, after two days; however once the silica was exhausted a switch of dominance was observed. Despite these are only preliminary

results, it provides important data necessary to discriminate the basic kinetic and physiological differences of the two organisms to help parametrize the model.

The importance of mixing events with periods of 5, 13, 24 and 120 hours are evident from the power spectra of turbulence (Figure 12). From the same figure, it is also evident that there is a higher energy for the lunar principal semidiurnal tidal mixing every 13 hours, and then there is comparable energy for the lunisolar diurnal tidal mixing and storm events every 24 and 120 hours. This information provided frequency of nutrient additions to test expected coccolithophore-diatom competition interaction in nature. Both the Monod and the mixed Droop-Monod models confirm the hypotheses that diatoms have an advantage in high turbulent mixing environments when nutrient pulse frequency reflects internal wave and tidal periods, from 5 to 24 hours. The coccolithophores when nutrient concentrations are low as observed in more stable aquatic environments, such as during summer at mid-latitude, as shown with the batch culture simulations. Coccolithophores also dominate with disturbance events every 120 hours, corresponding to the average storm occurrence in the ocean (Figure 20). The fact that diatoms have higher instantaneous growth rates at the moment of the pulse in long period mixing event does not affect the final result of coccolithophore dominance. A switch in dominance from diatom to coccolithophores occurs consistently as soon as the nitrate concentration runs below a critical value of $0.8 \mu\text{M}$ for the Monod model. The advantage of vacuole storage for the diatoms in highly nutrient-limiting conditions is evident in the mixed Droop-Monod numerical simulation. This advantage only lasts a few doublings, when the nutrient reserve is completely utilized. The numerical simulations confirm that competitive exclusion is faster in a steady system than in a pulsed one (Grover 1988).

These results can be interpreted in the context of two organisms with different niches and r and K selection strategies (MacArthur and Wilson, 1967). I had the niche as n -dimensional hypervolume where the organism lives and reproduces. I then had the diatoms as the opportunistic r strategist, adapted to a more variable environment with a faster potential growth rate. Viceversa coccolithophores are K strategist adapted to a more stable environment, with a lower potential growth rate. This approach cannot be fully adopted in the common notion of the r - K selection theory, because diatoms can reach the carrying capacity of they environment. Coccolithophores at the same time in comparison to the diatoms are not much bigger, and this is another divergence from the classical r - K selection theory assumptions

5 Prospect

The laboratory and numerical simulation experimental work supported the initial hypotheses of a selective effect of a variable resource environment on diatoms and coccolithophores' dominance and succession. The differences between the Monod and mixed Droop-Monod models showed mostly a quantitative but not a qualitative difference between resource competition of diatoms and coccolithophores. The final output of the different conditions tested did not vary, where instead there was a difference in critical nutrient concentrations at which switch of dominance was registered. The Droop model adopted for the diatoms in the mixed models resulted in a lower metabolism for this organism, with an advantage to keep a high growth rate in between short nutrient pulses. These results were produced believing that understanding the mechanisms that

lead to the succession of phytoplankton functional groups is essential to quantify the global carbon cycle dynamics. An increase in succession with the shifting of the ecosystem structure from diatom to coccolithophore-dominated communities has biogeochemical consequences. For these reason, it is critical to have a better understanding of succession and competition mechanisms between these two key functional phytoplankton groups.

These results also illustrate how reliable mathematical approaches help us understand marine phytoplankton successions which provide us with a tool to interpret observed changes in nature and will contribute to a better assessment of the likely impact of environmental change on natural populations of marine phytoplankton, and how these populations change in space and time.

Appendix (Source code)

Each model is composed of a main code, Monod.m and Droop.m, which calls 3 other functions and loads variables from two text files (vard.txt and pul.txt). The M0.m and D0.m functions contain the set of ordinary differential equations that are solved by the Matlab implemented ODE15s solver. The M2.m and D2.m functions back-calculates the cells' growth rates, and the dilution and nutrient dilution from the solver output. The nutrient pulse function, pulse1.m, is the same for the two models.

Monod model

Main code (Monod)

```
% Monod model for diatoms and coccolithophores
% Nitrogen based
% Sasha 15/07/2001 ver 0.0.0

% This file is calls functions MO, M2 and pulse1

clear all;
pack;
clc;

format long g;

a = load('vard.txt','r'); % Load physiological variables
b = load('pul.txt','r'); % Load pulse characteristic

df=a(1)/10; % dilution factor (d-1)
Vmax_D = a(2)/10; % diatoms maximum specific division rate (h-1)
Vmax_C = a(3)/10; % coccolithophores maximum specific division rate (h-1)
KN_D = a(4); % Diatom half saturation constant (μmol N ml-1)
KN_C = a(5); % Coccolithophores half saturation constant (μmol N ml-1)

odeset('MaxStep', 0.25);
% odeset ('NormControl', 'on');
odeset ('RelTol' , 1e-5);

D=input('Starting diatom cell density (cell ml-1):'); % Starting diatom cell density (cell ml-1)
C=input('Starting coccolithophore cell density (cell ml-1):'); % Starting coccolithophore cell density (cell ml-1)
N=input('Starting N concentration (μmol N ml-1):'); % Starting N concentration (μmol N ml-1)
ht=input('Hours of run (h):'); % Hours of run (h)
idrun = input('ID Run:','s');

h=ht*10;

[t, y] = ode15s('M0', 1:h, [D, C, N]);
```

```

X = M2(y);
M = [y X];

% Output

fid1=fopen([idrun '.txt'], 'w');
fprintf(fid1, '%6.0f %6.0f %6.0f %6.0f %6.0f %6.2f %6.2f %6.0f\n', M);
fclose(fid1);

% Graph

figure(1);
set(1,...
    'Name','Monod Competition Model',...
    'NumberTitle','Off',...
    'MenuBar','None');

mout = M';

clf

X1=t/10; % Time (h)
Y1=mout(1,:); % Diatom density (cell ml-1)
Y2=mout(2,:); % Coccolithophores density (cell ml-1)
Y3=mout(3,:); % N concentration (μmol N ml-1)
Y4=mout(8,:); % N input and dilution
Y5=mout(4,:); % Diatom μ (h-1)
Y6=mout(5,:); % Coccolithophore μ (h-1)

subplot(4,1,1);
handl=semilogy(X1,Y1,'g-',X1,Y2,'r-');
set(gca, 'FontSize', 7);
set(handl,'LineWidth',1);
set(handl,'MarkerSize',7);
grid off;
y1max=ylim;
y1max=y1max(2);
axis([0 h/10 0 y1max]);
ylabel('Cell ml-1', 'FontSize',7);
legend('Diatoms','Coccolithophores');
title('Monod model for Diatoms & Coccolithophores','FontSize',7);

subplot(4,1,2);
handl=plot(X1,Y3,'b-');
set(gca, 'FontSize', 7);
set(handl,'LineWidth',1);
set(handl,'MarkerSize',7);
grid off
y2max=ylim;
y2max=y2max(2);
axis([0 h/10 0 y2max]);
ylabel('NO3 (μM)', 'FontSize',7);

subplot(4,1,3);
handl=plot(X1,Y5,'g:',X1,Y6,'r:');
set(gca, 'FontSize', 7);
set(handl,'LineWidth',1);
set(handl,'MarkerSize',7);
grid off
y2max=ylim;
y2max=y2max(2);

```

```

axis([0 h/10 0 y2max]);
ylabel('\mu (h^{-1})','FontSize',7);
legend('Diatoms \mu ','Coccolithophores \mu');

subplot(4,1,4);
handl=plot(X1,Y4,'k-');
set(gca, 'FontSize', 7);
set(handl,'LineWidth',1);
set(handl,'MarkerSize',7);
grid off
y2max=ylim;
y2max=y2max(2);
axis([0 h/10 0 y2max]);
ylabel('NO_3 (\mu M)','FontSize',7);
xlabel('Time (h)','FontSize',7);

str1 = num2str(b(1));
str2 = num2str(b(2));
str3 = num2str(b(3));
str4 = num2str(b(4));

axes('position',[0 0 1 1],'visible','off');
text(0,0,'Pulse Period:',...           % Lower Left Graph Comment
     'FontSize', 7,...
     'horizontalalignment','left',...
     'verticalalignment','bottom');
text(0.10,0,str1,...                   % Lower Left Graph Comment
     'FontSize', 7,...
     'horizontalalignment','left',...
     'verticalalignment','bottom');
text(0.15,0,'(h)',...                 % Lower Left Graph Comment
     'FontSize', 7,...
     'horizontalalignment','left',...
     'verticalalignment','bottom');

text(0.2,0,'Pulse Lenght:',...         % Lower Center Graph Comment
     'FontSize', 7,...
     'horizontalalignment','left',...
     'verticalalignment','bottom');
text(0.32,0,str2,...                   % Lower Center Graph Comment
     'FontSize', 7,...
     'horizontalalignment','left',...
     'verticalalignment','bottom');
text(0.34,0,'(h)',...                 % Lower Center Graph Comment
     'FontSize', 7,...
     'horizontalalignment','left',...
     'verticalalignment','bottom');

text(0.38,0,'Pulse Intensity:',...     % Lower Center Graph Comment
     'FontSize', 7,...
     'horizontalalignment','left',...
     'verticalalignment','bottom');
text(0.52,0,str3,...                   % Lower Center Graph Comment
     'FontSize', 7,...
     'horizontalalignment','left',...
     'verticalalignment','bottom');
text(0.55,0,'(\mu mol N ml^{-1})',... % Lower Center Graph Comment
     'FontSize', 7,...
     'horizontalalignment','left',...
     'verticalalignment','bottom');

text(0.68,0,'Backgroud N input:',...   % Lower Right Graph Comment

```

```

    'FontSize', 7,...
    'horizontalalignment','left',...
    'verticalalignment','bottom');
text(0.83,0,str4,...           % Lower Right Graph Comment
    'FontSize', 7,...
    'horizontalalignment','left',...
    'verticalalignment','bottom');
text(0.87,0,'(μmol N ml-1)',...   % Lower Right Graph Comment
    'FontSize', 7,...
    'horizontalalignment','left',...
    'verticalalignment','bottom');

saveas(gcf, [idrun '.fig']);
fclose('all');

```

Function M0

```

function [derivative] = M0(t,y)

% Monod model for diatoms and coccolithophores
% Nitrogen based
% Sasha 15/07/2001 ver 0.0.0

format long g;

a = load('vard.txt','r'); % Load physiological variables
b = load('pul.txt','r'); % Load pulse characteristic

df=a(1)/10;           % dilution factor (d-1)
Vmax_D = a(2)/10;    % diatoms maximum specific division rate (h-1)
Vmax_C = a(3)/10;    % coccolithophores maximum specific division rate (h-1)
KN_D = a(4);         % Diatom half saturation constant (μmol N ml-1)
KN_C = a(5);         % Coccolithophores half saturation constant (μmol N ml-1)

QD = a(12);          % Diatom yield coefficient (cell μmol N-1)
QC = a(11);          % Coccolithophore yield coefficient (cell μmol N-1)

Period = b(1)*10;
PulseOnFor = b(2)*10;

Nin= b(4) + pulse1(t,PulseOnFor,Period)*(b(3)-b(4));

DN=(Nin-y(3))*df;      % N dilution
DD=y(1)*df;           % diatom dilution
DC=y(2)*df;           % coccolithophore dilution
VD=(Vmax_D*y(3))/(KN_D+y(3)); % diatom μ (h-1)
VC=(Vmax_C*y(3))/(KN_C+y(3)); % coccolithophore μ (h-1)
d(1)=y(1)*VD-DD;      % diatom cell density (cell ml-1)
d(2)=y(2)*VC-DC;      % coccolithophore cell density (cell ml-1)
d(3)= DN-((VD*y(1))/QD)-((VC*y(2))/QC); % N concentration (μmol N ml-1)

derivative = d';

```

Function M2

```

function [X]=M2(y);

```

```

% This function is called by Monod.m
% Back calculates VC, VD, DD, DC, DN
% Sasha Tozzi 15/07/2001 Ver 0.0.0

format long g;

a = load('vard.txt','r'); % Load physiological variables
b = load('pul.txt','r'); % Load pulse characteristic

df=a(1)/10; % dilution factor (d-1)
Vmax_D = a(2)/10; % diatoms maximum specific division rate (h-1)
Vmax_C = a(3)/10; % coccolithophores maximum specific division rate (h-1)
KN_D = a(4); % Diatom half saturation constant (μmol N ml-1)
KN_C = a(5); % Coccolithophores half saturation constant (μmol N ml-1)

Period = b(1)*10;
PulseOnFor = b(2)*10;

len = length(y);

X=[];

for ii=1:len

Nin = b(4) + pulse1(ii,PulseOnFor,Period)*(b(3)-b(4));

DN=(Nin-y(ii,3))*df; % N dilution
DD=y(ii,1)*df; % diatom dilution
DC=y(ii,2)*df; % coccolithophore dilution
VD=(Vmax_D*y(ii,3))/(KN_D+y(ii,3)); % diatom μ (h-1)
VC=(Vmax_C*y(ii,3))/(KN_C+y(ii,3)); % coccolithophore μ (h-1)

X = [X; VD VC DD DC DN];

End

```

Function Pulse1

```

% Monod model for diatoms and coccolithophores
% Nitrogen based
% Sasha 17/07/2001 ver 0.0.0

function result=pulse1(t,onfor,T)

% this will be an on/off pulse with a gradual increase and decrease
% rather than a purely on-off function.

width = onfor/10;
result=0.0;
reducedt = mod(t,T);

if (reducedt<=onfor)
    if (reducedt < width)
        result = reducedt*width;
    else if ( T-reducedt < width)
        result = (T-reducedt)*width;
    else
        result = 1.0;
    end
end

```

```
end
end
```

Mixed Droop-Monod model

Main code (Droop)

```
% Mix Droop-Monod model for diatoms and coccolithophores
% Nitrogen based
% Sasha 17/07/2001 ver 0.0.1

% This file is calls functions DO and D2

clear all;
pack;
clc;

format long g;

a = load('vard.txt','r'); % Load physiological variables
b = load('pul.txt','r'); % Load pulse characteristic

df=a(1)/10; % dilution factor (d-1)
Vmax_D = a(2)/10; % diatoms maximum specific division rate (h-1)
Vmax_C = a(3)/10; % coccolithophores maximum specific division rate (h-1)
KN_D = a(4); % Diatom half saturation constant ( $\mu\text{mol N ml}^{-1}$ )
KN_C = a(5); % Coccolithophores half saturation constant ( $\mu\text{mol N ml}^{-1}$ )
Amax_N_D = a(6)/10; % Diatom maximal uptake rate for N ( $\mu\text{mol N cell}^{-1} \text{ h}^{-1}$ )
Qmin_N_D = a(7); % Minimal diatom N cell quota ( $\mu\text{mol N cell}^{-1}$ )
Qmax_N_D = a(8); % Maximal diatom N cell quota ( $\mu\text{mol N cell}^{-1}$ )
QND = a(9); % Starting diatom N cell quota ( $\mu\text{mol N cell}^{-1}$ )
Kq_N_D = a(10); % Diatom half saturation constant for cell quota ( $\mu\text{mol N cell}^{-1}$ )

% odeset('MaxStep', 0.25);
% odeset('NormControl', 'on');
% odeset('RelTol', 1e-5);

D=input('Starting diatom cell density (cell ml-1):'); % Starting diatom cell density (cell ml-1)
C=input('Starting coccolithophore cell density (cell ml-1):'); % Starting coccolithophore cell density (cell ml-1)
N=input('Starting N concentration ( $\mu\text{mol N ml}^{-1}$ ):'); % Starting N concentration ( $\mu\text{mol N ml}^{-1}$ )
ht=input('Hours of run (h):'); % Hours of run (h)
idrun = input('ID Run:','s');

h=ht*10;

[t, y] = ode15s('D0', 1:h, [ D, C, N, QND]);

X = D2(y);
M = [y X];

% Output

fid1=fopen([idrun '.txt'], 'w');
fprintf(fid1, '%6.0f %6.0f %6.0f %6.0f %6.2f %6.2f %6.2f %6.2f %6.0f\n', M');
fclose(fid1);

% Graph
```

```

figure(1);
set(1,...
    'Name','Mix Droop-Monod Competition Model',...
    'NumberTitle','Off',...
    'MenuBar','None');

dout = M';

clf

X1=t/10;          % Time (h)
Y1=dout(1,:);     % Diatom density (cell ml-1)
Y2=dout(2,:);     % Coccolithophores density (cell ml-1)
Y3=dout(3,:);     % N concentration (μmol N ml-1)
Y4=dout(10,:);    % N concentration (μmol N ml-1)
Y5=dout(5,:);     % Diatom μ (h-1)
Y6=dout(6,:);     % Coccolithophore μ (h-1)

subplot(4,1,1);
handl=semilogy(X1,Y1,'g-',X1,Y2,'r-');
set(gca, 'FontSize', 7);
set(handl,'LineWidth',1);
set(handl,'MarkerSize',7);
grid off;
y1max=ylim;
y1max=y1max(2);
axis([0 h/10 0 y1max]);
ylabel('Cell ml-1','FontSize',7);
legend('Diatoms','Coccolithophores');
title('Mix Droop-Monod model for Diatoms & Coccolithophores','FontSize',7);

subplot(4,1,2);
handl=plot(X1,Y3,'b-');
set(gca, 'FontSize', 7);
set(handl,'LineWidth',1);
set(handl,'MarkerSize',7);
grid off;
y2max=ylim;
y2max=y2max(2);
axis([0 h/10 0 y2max]);
ylabel('NO3 (μM)','FontSize',7);

subplot(4,1,3);
handl=plot(X1,Y5,'g:',X1,Y6,'r:');
set(gca, 'FontSize', 7);
set(handl,'LineWidth',1);
set(handl,'MarkerSize',7);
grid off;
y2max=ylim;
y2max=y2max(2);
axis([0 h/10 0 y2max]);
ylabel('μ (h-1)','FontSize',7);
legend('Diatoms μ ','Coccolithophores μ');
xlabel('Time (h)','FontSize',7);

subplot(4,1,4);
handl=plot(X1,Y4,'k-');
set(gca, 'FontSize', 7);
set(handl,'LineWidth',1);
set(handl,'MarkerSize',7);
grid off

```

```

y2max=ylim;
y2max=y2max(2);
axis([0 h/10 0 y2max]);
ylabel('NO_3 (\mu M)', 'FontSize', 7);
xlabel('Time (h)', 'FontSize', 7);

str1 = num2str(b(1));
str2 = num2str(b(2));
str3 = num2str(b(3));
str4 = num2str(b(4));

axes('position',[0 0 1 1], 'visible', 'off');
text(0,0,'Pulse Period:',...           % Lower Left Graph Comment
     'FontSize', 7,...
     'horizontalalignment','left',...
     'verticalalignment','bottom');
text(0.12,0,str1,...                    % Lower Left Graph Comment
     'FontSize', 7,...
     'horizontalalignment','left',...
     'verticalalignment','bottom');
text(0.15,0,'(h)',...                  % Lower Left Graph Comment
     'FontSize', 7,...
     'horizontalalignment','left',...
     'verticalalignment','bottom');

text(0.2,0,'Pulse Lenght:',...          % Lower Center Graph Comment
     'FontSize', 7,...
     'horizontalalignment','left',...
     'verticalalignment','bottom');
text(0.32,0,str2,...                   % Lower Center Graph Comment
     'FontSize', 7,...
     'horizontalalignment','left',...
     'verticalalignment','bottom');
text(0.34,0,'(h)',...                  % Lower Center Graph Comment
     'FontSize', 7,...
     'horizontalalignment','left',...
     'verticalalignment','bottom');

text(0.38,0,'Pulse Intensity:',...      % Lower Center Graph Comment
     'FontSize', 7,...
     'horizontalalignment','left',...
     'verticalalignment','bottom');
text(0.52,0,str3,...                   % Lower Center Graph Comment
     'FontSize', 7,...
     'horizontalalignment','left',...
     'verticalalignment','bottom');
text(0.55,0,'(\mu mol N ml-1)',...      % Lower Center Graph Comment
     'FontSize', 7,...
     'horizontalalignment','left',...
     'verticalalignment','bottom');

text(0.68,0,'Backgroud N input:',...    % Lower Right Graph Comment
     'FontSize', 7,...
     'horizontalalignment','left',...
     'verticalalignment','bottom');
text(0.82,0,str4,...                   % Lower Right Graph Comment
     'FontSize', 7,...
     'horizontalalignment','left',...
     'verticalalignment','bottom');
text(0.87,0,'(\mu mol N ml-1)',...      % Lower Right Graph Comment
     'FontSize', 7,...
     'horizontalalignment','left',...

```



```

    'verticalalignment','bottom');

    saveas(gcf, [idrun '.fig']);

    fclose('all');

```

Function D0

```

function [derivative] = D0(t,y)

% Mix Droop-Monod model for diatoms and coccolithophores
% Nitrogen based
% Sasha 17/07/2001 ver 0.0.1

format long g;

a=load('vard.txt','r'); % Load physiological variables
b=load('pul.txt','r'); % Load pulse characteristic

df=a(1)/10; % dilution factor (d-1)
Vmax_D = a(2)/10; % diatoms maximum specific division rate (h-1)
Vmax_C = a(3)/10; % coccolithophores maximum specific division rate (h-1)
KN_D = a(4); % Diatom half saturation constant (μmol N ml-1)
KN_C = a(5); % Coccolithophores half saturation constant (μmol N ml-1)
Amax_N_D = a(6)/10; % Diatom maximal uptake rate for N (μmol N cell-1 h-1)
Qmin_N_D = a(7); % Minimal diatom N cell quota (μmol N cell-1)
Qmax_N_D = a(8); % Maximal diatom N cell quota (μmol N cell-1)
QND = a(9); % Starting diatom N cell quota (μmol N cell-1)
Kq_N_D = a(10); % Diatom half saturation constant for cell quota (μmol N cell-1)
QC = a(11); % Coccolithophore yield coefficient (cell μmol N-1)

Period = b(1)*10;
PulseOnFor = b(2)*10;

Nin= b(4) + pulse1(t,PulseOnFor,Period)*(b(3)-b(4)); % ~ background N + pulse N

% Diatom N uptake (μmol N cell-1 h-1)

A_N_D = ((Amax_N_D*y(3))/(KN_D+y(3)));
%A_N_D = ((Amax_N_D*y(3))/(KN_D+y(3)))*((Qmax_N_D-y(4))/(Qmax_N_D-Qmin_N_D)); % Alternative

    if A_N_D < 0
        A_N_D = 0;
    end;

DN = (Nin-y(3))*df; % N dilution
DD = y(1)*df; % Diatom dilution
DC = y(2)*df; % Coccolithophore dilution
VD = Vmax_D*((y(4)-Qmin_N_D)/(y(4))); % Diatom μ (h-1)
%VD=Vmax_D*((y(4)-Qmin_N_D)/(Kq_N_D + y(4)-Qmin_N_D)); % Alternative diatom μ (h-1)
VC = (Vmax_C*y(3))/(KN_C+y(3)); % Coccolithophore μ (h-1)
d(1)= y(1)*VD-DD; % Diatom cell density (cell ml-1)
d(2)= y(2)*VC-DC; % Coccolithophore cell density (cell ml-1)
d(3)= DN-(A_N_D*y(1))-(VC*y(2)/QC); % N concentration (μmol N ml-1)
d(4)= A_N_D-VD*y(4); % Diatom N cell quota (μmol N cell-1)

derivative = d';

```

Function D2

```

function [derivative] = D2(y)

% This function back calculates uptake, dilutions and  $\mu$ 
% Mix Droop-Monod model for diatoms and coccolithophores
% Nitrogen based
% Sasha 17/07/2001 ver 0.0.1

format long g;

a=load('vard.txt','r'); % Load physiological variables
b = load('pul.txt','r'); % Load pulse characteristic

df=a(1)/10; % dilution factor (d-1)
Vmax_D = a(2)/10; % diatoms maximum specific division rate (h-1)
Vmax_C = a(3)/10; % coccolithophores maximum specific division rate (h-1)
KN_D = a(4); % Diatom half saturation constant ( $\mu\text{mol N ml}^{-1}$ )
KN_C = a(5); % Coccolithophores half saturation constant ( $\mu\text{mol N ml}^{-1}$ )
Amax_N_D = a(6)/10; % Diatom maximal uptake rate for N ( $\mu\text{mol N cell}^{-1} \text{ h}^{-1}$ )
Qmin_N_D = a(7); % Minimal diatom N cell quota ( $\mu\text{mol N cell}^{-1}$ )
Qmax_N_D = a(8); % Maximal diatom N cell quota ( $\mu\text{mol N cell}^{-1}$ )
QND = a(9); % Starting diatom N cell quota ( $\mu\text{mol N cell}^{-1}$ )
Kq_N_D = a(10); % Diatom half saturation constant for cell quota ( $\mu\text{mol N cell}^{-1}$ )

Period = b(1)*10;
PulseOnFor = b(2)*10;

len = length(y);

X=[];

for ii=1:len

% Diatom N uptake ( $\mu\text{mol N cell}^{-1} \text{ h}^{-1}$ )

    A_N_D = ((Amax_N_D*y(ii,3))/(KN_D+y(ii,3)));

    if A_N_D < 0
        A_N_D = 0;
    end;

    Nin= b(4) + pulse1(ii,PulseOnFor,Period)*(b(3)-b(4));

    DN=(Nin-y(ii,3))*df; % N dilution
    DD=y(ii,1)*df; % Diatom dilution
    DC=y(ii,2)*df; % Coccolithophore dilution
    %VD=Vmax_D*((y(ii,4)-Qmin_N_D)/(Kq_N_D + y(ii,4)-Qmin_N_D)); % Alternative diatom  $\mu$  (h-1)
    VD=Vmax_D*((y(ii,4)-Qmin_N_D)/(y(ii,4))); % Diatom  $\mu$  (h-1)
    VC=(Vmax_C*y(ii,3))/(KN_C+y(ii,3)); % Coccolithophore  $\mu$  (h-1)

    X = [X; VD VC DD DC A_N_D DN];

derivative=X;

end

```

Bibliography

- Arrigo, K.R. and Sullivan, C.W., 1992. The influence of salinity and temperature covariation on the photophysiological characteristic of antarctica sea ice microalgae. *Journal of Phycology*, 28: 746-756.
- Balch, W.M., Kilpatrick, K.A., Holligan, P., Harbour, D. and Fernandez, E., 1996a. The 1991 coccolithophore bloom in the central North Atlantic .2. Relating optics to coccolith concentration. *Limnology and Oceanography*, 41(8): 1684-1696.
- Balch, W.M., Kilpatrick, K.A. and Trees, C.C., 1996b. The 1991 coccolithophore bloom in the central North Atlantic .1. Optical properties and factors affecting their distribution. *Limnology and Oceanography*, 41(8): 1669-1683.
- Begon, M., J. Harper, et al. (1986). *Ecology*, Blackwell Scientific.
- Bienfang, P. K. 1985. Size structure and sinking rates of various microparticulate constituents in oligotrophic Hawaiian waters. *Mar. Ecol. Prog. Ser.*, **23**: 143-151.
- Bienfang, P. K., P. J. Harrison, and L. M. Quarmby. 1982. Sinking rate response to depletion of nitrate, phosphate and silicate in four marine diatoms. *Mar. Biol.* **67**: 295-302.
- Bishop, J.K.B., 1989. Regional Extremes in Particulate Matter Composition and Flux: Effects on the Chemistry of the Ocean Interior. In: W.H. Berger, V.S. Smetacek and G. Wefer (Editors), *Productivity of the Ocean: Present and Past*. Life Science Research Report. Wiley, Chichester, pp. 117-137.
- Boyd, P.W. et al., 2000. A mesoscale phytoplankton bloom in the polar Southern Ocean stimulated by iron fertilization. *Nature*, 407(6805): 695-702.
- Brand, L.E., 1982. Genetic variability and spatial patterns of genetic differentiation in the reproductive rates of the marine coccolithophores *Emiliana huxleyi* and *Gephyrocapsa oceanica*. *Limnology and Oceanography*, 27(2): 236-245.
- Brand, L.E., 1994. Physiological ecology of marine coccolithophores.
- Brand, L.E. and Guillard, R.R.L., 1981. The Effects of Continuous Light and Light Intensity on the Reproduction Rates of Twenty-Two Species of Marine Phytoplankton. *J. Exp. Mar. Biol. Ecol.*, 50: 2-3.
- Bratbak, G. et al., 1995. Viral activity in relation to *Emiliana huxleyi* blooms: A mechanism of DMSP release? *Marine Ecology-Progress Series*, 128(1-3): 133-142.
- Brzezinski, M.A., 1985. The Si:C:N ratio of marine diatoms: Interspecific variability and the effect of some environmental variables. *J. Phycol.*, 21(3): 347-357.
- Busby, W.F. and Lewin, J., 1967. Silicate uptake and Silica shell formation formation by synchronously dividing cell of the diatom *Navicula pelliculosa* (Bréb.) Hilse. *Journal of Phycology*, 3: 127-131.
- Chisholm, S.W., Morel, F.M.M. and Slocum, W.S., 1980. The phasing and distribution of cell division. In: P.G. Falkowski (Editor), *Primary Productivity in the Sea*. Environmental Science Research. Plenum Press, NY, pp. 281-300.

- Cloern, J.E., 1977. Effect of light intensity and temperature on *Cryptomonas ovata* (Crptophyceae) growth and nutrient uptake rates. *Journal of Phycology*, 13: 389-395.
- Connel, J.H. and Slatyer, R.O., 1977. Mechanism of succession in natural communities and their role in community stability and organization. *The American Naturalist*, 111(982): 1119-1144.
- Connel, J.H., 1978. Diversity in Tropical Rain Forests and Coral Reefs. *Science*, 199: 1302-1310.
- Cullen, J.J., Yang, X. and MacIntyre, H.L., 1992. Nutrient limitation of marine photosynthesis. In: P.G. Falkowski and A.D. Woodhead (Editors), *Primary Productivity and Biogeochemical Cycles in the Sea*. Plenum Press, New York, pp. 69-88.
- Daly, K.L. and Smith, W.O.J., 1993. Physical-Biological Interactions Influencing Marine Plankton Production. *Annual Review of Ecology and Systematics*, 24: 555-585.
- Davidson, K. and Gurney, W.S.C., 1999. An investigation of non-steady-state algal growth. II. Mathematical modelling of co-nutrient-limited algal growth. *Journal of Plankton Research*, 21(5): 839-858.
- Davidson, K., Wood, G., John, E.H. and Flynn, K.J., 1999. An investigation of non-steady-state algal growth. I. An experimental model ecosystem. *Journal of Plankton Research*, 21(5): 811-837.
- De La Rocha, C.L., Hutchins, D.A., Brzezinski, M.A. and Zhang, Y.H., 2000. Effects of iron and zinc deficiency on elemental composition and silica production by diatoms. *Marine Ecology-Progress Series*, 195: 71-79.
- Delwiche, C.F., 1999. Tracing the thread of plastid diversity through the tapestry of life. *American Naturalist*, 154: S164-S177.
- Droop, M.R., 1973. Some thoughts on nutrient limitation in algae. *Journal of Phycology*, 9: 264-272.
- Dugdale, R.C. and Wilkerson, F.P., 1998. Silicate regulation of new production in the equatorial Pacific upwelling. *Nature*, 391: 270-273.
- Egge, J.K. and Aksnes, D.L., 1992. Silicate as regulating nutrient in phytoplankton competition. *Mar. Ecol. Prog. Ser.*, 83: 281-289.
- Eppley, R.W., 1972. Temperature and phytoplankton growth in the sea. *Fisheries Bulletin*, 70: 1063-1085.
- Eppley, R.W. and Peterson, B.J., 1979. Particulate organic matter flux and planktonic new production in the deep ocean. *Nature*, 286: 677-680.
- Eppley, R.W., Rogers, J.N., McCarthy, J.J. and Sournia, A., 1971. Light/Dark periodicity in nitrogen assimilation of the marine phytoplankters *Skeletonemacostatum* and *Coccolithus huxleyi* in N-limited chemostat culture. *Journal of Phycology*, 7: 150-154.
- Eppley, R.W., Rogers, J.N. and McCarthy, J.J., 1969. Half-Saturation constant for uptake of nitrate and ammonium by marine phytoplankton. *Limnology and Oceanography*, 14: 912-920.
- Falkowski, P.G., 1981. Light-shade adaptation and assimilation numbers. *Journal of Plankton Research*, 3(2): 203-216.
- Falkowski, P.G., 1997. Evolution of the nitrogen cycle and its influence on the biological sequestration of CO₂ in the ocean. *Nature*, 387(6630): 272-275.

- Falkowski, P.G. and Raven, J.A., 1997. Aquatic photosynthesis, 375 pp.
- Fernández, E., Fritz, J.J. and Balch, W.M., 1996. Chemical composition of the coccolithophorid *Emiliania huxleyi* under light-limited steady state growth. *Journal of Experimental Marine Biology and Ecology*, 207(1-2): 149-160.
- Finlay, B.J., Maberly, S.C. and Cooper, I., 1997. Microbial diversity and ecosystem function. *Oikos*, 80: 209-213.
- Fisher, T.R. and Butt, A.J., 1994. The Role of Nitrogen and Phosphorus in Chesapeake Bay Anoxia. In: S. Nelson and P. Elliot (Editors), *Perspectives on Chesapeake Bay, 1994. Advances in Estuarine Sciences. Chesapeake Bay Program's Scientific and Technical Advisory Committee (STAC)*.
- Flynn, K.J. and Hipkin, C.R., 1999. Interactions between iron, light, ammonium, and nitrate: Insights from the construction of a dynamic model of algal physiology. *Journal of Phycology*, 35: 1171-1190.
- Gao, Y., Kaufman, Y.J., Tanre, D., Kolber, D. and Falkowski, P.G., 2001. Seasonal distributions of aeolian iron fluxes to the global ocean. *Geophysical Research Letters*, 28(1): 29-32.
- Geider, R.J., 1999. Biological oceanography - Complex lessons of iron uptake. *Nature*, 400(6747): 815-816.
- Goldman, J.C., 1977. Steady state, growth of phytoplankton in continuous culture: comparison of internal and external nutrient equation. *Journal of Phycology*, 13: 251-258.
- Goldman, J.C. and Ryther, J.H., 1976. Temperature species competition in mass cultures of marine influenced phytoplankton. *Biotechnol. Bioengng*, 18: 1125-44.
- Grasshoff, K., 1976. *Methods of seawater analysis*, New York, 317 pp.
- Green, R.M., Geider, R.J. and Falkowski, G.P., 1991. Effect of iron limitation on photosynthesis in a marine diatom. *Limnology and Oceanography*, 36(8): 1772-1782.
- Grover, J.P., 1988. Dynamics of Competition in a Variable Environment: Experiments with Two Diatom Species. *Ecology*, 69(2): 408-417.
- Grover, J.P., 1989. Phosphorus-dependent growth kinetics of 11 species of freshwater algae. *Limnol. Oceanogr.*, 34(2): 341-348.
- Guillard, R.R.L., 1975. Culture of phytoplankton for feeding marine invertebrates. In: W.L.S.a.M.H. Chanley (Editor), *Culture of Marine Invertebrate Animals*. Plenum Press, New York, pp. 26-60.
- Guillard, R.R.L. and Ryther, J.H., 1962. Studies of marine planktonic diatoms. I. *Cyclotella nana* Hustedt and *Detonula confervacea* Cleve. *Can. J. Microbiol.*, 8: 229-239.
- Haidar, A. T., H. R. Thierstein, Deuser, W. G. 2000. Calcareous phytoplankton standing stocks, fluxes and accumulation in Holocene sediments off Bermuda (N. Atlantic). *Deep Sea Research Part II: Topical Studies in Oceanography* 47(9-11): 1907-1938
- Hallegraeff, G.M., 1993. A review of harmful algal blooms and their apparent global increase. *Phycologia*, 32(2): 79-99.
- Hein, M. and Riemann, B., 1995. Nutrient Limitation of Phytoplankton Biomass or Growth-Rate - an Experimental Approach Using Marine Enclosures. *Journal of Experimental Marine Biology and Ecology*, 188(2): 167-180.

- Holligan, P.M. and Robertson, J.E., 1996. Significance of ocean carbonate budgets for the global carbon cycle. *Global Change Biology*, 2(2): 85-95.
- Huisman, J. and Weissing, F.J., 1999. Biodiversity of plankton by species oscillations and chaos. *Nature*, 402: 407-410.
- Hulburt, E.M., 1970. Competition for nutrients by marine phytoplankton in oceanic, coastal, and estuarine regions. *Ecology*, 51(3): 475-484.
- Hulburt, E.M. and Horton, D., 1973. Minimum interferences between plankton species and its beneficial effect. *Marine Biology*, 23: 35-8.
- Hutchins, D.A. and Bruland, K.W., 1998. Iron-limited diatom growth and Si:N uptake ratios in a coastal upwelling regime. *Nature*, 393: 561-564.
- Hutchinson, G.E., 1961. The paradox of the plankton. *American Naturalist*, 95: 137-145.
- Kirk, J.T.O., 1983. *Light and Photosynthesis in Aquatic Ecosystems*. Cambridge Univ. Press, Cambridge, 401 pp.
- Kolber, Z., Prasil, O. and Falkowski, P.G., 1998. Measurements of variable chlorophyll fluorescence using fast repetition rate techniques: defining methodology and experimental protocols. *Biochimica et Biophysica Acta*, 1367: 88-106.
- Lewis, M.R., Horne, E.P.W., Cullen, J.J., Oakey, N.S. and Platt, T., 1984. Turbulent mixing may control photosynthesis in the upper ocean. *Nature*, 311(5981): 49-50.
- Li, W.K.W., 1985. Photosynthetic response to temperature of marine phytoplankton along a latitudinal gradient (16°N to 74°N). *Deep-Sea Research*, 32(11): 1381-1391.
- Litchman, E. and Klausmeier, C.A., 2001. Competition of phytoplankton under fluctuating light. *American Naturalist*, 157(2): 170-187.
- Longhurst, A.R. and Harrison, W.C., 1989. The biological pump: profiles of plankton production and consumption in the upper ocean. *Progress in Oceanography*, 22: 47-123.
- Margalef, R., 1960. Temporal succession and spatial heterogeneity in phytoplankton. In: A.A. Buzzati-Traverso (Editor), *Perspectives in marine biology*. University of California Press, Berkeley, pp. 323-349.
- Margalef, R., 1997. *Our Biosphere. Excellence in ecology*, 10. Ecology Institute, Oldendorf, 176 pp.
- Mitchell, B.G., Brody, E.A., Holm-Hansen, O., McClain, C. and Bishop, J., 1991. Light limitation of phytoplankton biomass and macronutrient utilization in the Southern Ocean. *Limnology and Oceanography*, 36(8): 1662-1677.
- Monod, J., 1950. La technique de la culture continue: theorie et applications. *Ann. Ist. Pasteur Lille* 390-410.
- Morel, A., 1991. Light and marine photosynthesis: a spectral model with geochemical and climatological implications. *Progress in Oceanography*, 26: 263-306.
- Morin, P.J., 1999. *Community Ecology*. Blackwell Science, Malden, 424 pp.
- Muggli, D.L. and Harrison, P.J., 1996. Effects of nitrogen source on the physiology and metal nutrition of *Emiliania huxleyi* grown under different iron and light conditions. *Marine Ecology Progress Series*, 130: 255-267.
- Muggli, D.L. and Harrison, P.J., 1997. Effects of iron on two oceanic phytoplankton grown in natural NE subArctic Pacific seawater with no artificial chelators present. *Journal of Experimental Marine Biology and Ecology*, 212(2): 225-237.

- Muggli, D.L., Lecourt, M. and Harrison, P.J., 1996. Effects of iron and nitrogen source on the sinking rate, physiology and metal composition of an oceanic diatom from the subarctic Pacific. *Marine Ecology Progress Series*, 132(1-3): 215-227.
- Nelson, D.M. and Brand, L.E., 1979. Cell division periodicity in 13 species of marine phytoplankton on a light:dark cycle. *Journal of Phycology*, 15: 65-75.
- Olsen, S. and Paasche, E., 1986. Variable Kinetics of Silicon -limited Growth in *Thalassiosira pseudonana* (Bacillariophyceae) in Response to Changed Chemical Composition of the Growth Medium. *British phycology Journal*, 21(183-190).
- Paasche, E., 1967. Marine Plankton Algae Grown with Light-Dark Cycles, I. *Coccolithus huxleyi*. *Physiologia Plantarum*, 20: 946-956.
- Paasche, E., 1973. Silicon and the Ecology of Marine Plankton Diatoms. I. *Thalassiosira pseudonana* (Cyclotella nana) Grown in a Chemostat with Silicate as Limiting Nutrient. *Marine Biology*, 19: 117-126.
- Paasche, E., 1980. Silicon content of five marine plankton diatom species measured with a rapid filter method. *Limnol. Oceanogr.*, 25(3): 474-480.
- Parsons, T.R., 1973. Coulter Counter for phytoplankton. In: J.R. Stein (Editor), *Handbook of Phycological Methods - Culture Methods and Growth Measurements*. Cambridge University Press, pp. 345-358.
- Patten, B.C. and Jorgensen, S.E., 1995. *Complex Ecology*. Prentice Hall PTR, Englewood, NJ, 705 pp.
- Payne, C.D. and Price, N.M., 1999. Effects of cadmium toxicity on growth and elemental composition of marine phytoplankton. *Journal of Phycology*, 35(2): 293-302.
- Petersen, R., 1975. The paradox of the plankton: an equilibrium hypothesis. *The American Naturalist*, 109(965): 35-49.
- Peterson, D.H., Perry, M.J., Bencala, K.E. and Talbot, M.C., 1987. Phytoplankton Productivity in Relation to Light Intensity: A Simple Equation. *Estuarine, Coastal and Shelf Science*, 24: 813-832.
- Platt, T., 1986. Primary production of the ocean column as a function of surface light intensity: algorithms for remote sensing. *Deep Sea Research*, 33(2): 149-163.
- Platt, T. and Jassby, A.D., 1976. The relationship between photosynthesis and light for natural assemblages of coastal marine phytoplankton. *Journal of Phycology*, 12: 421-430.
- Raven, J.A., 1997. The vacuole: A cost-benefit analysis. *Advances in Botanical Research Incorporating Advances in Plant Pathology*, Vol 25, 25: 59-86.
- Reynolds, C.S., 1976. Succession and Vertical Distribution of Phytoplankton in Response to Thermal Stratification in a Lowland Mere, with Special Reference to Nutrient Availability. *Journal of Ecology*, 64(2): 529-551.
- Riegman, R., Stolte, W., Noordeloos, A.A.M. and Slezak, D., 2000. Nutrient uptake and alkaline phosphatase (EC 3:1:3:1) activity of *Emiliania huxleyi* (Prymnesiophyceae) during growth under N and P limitation in continuous cultures. *J. Phycol.*, 36(1): 87-96.
- Ryther, J.H., 1956. Photosynthesis in the Ocean as a Function of Light Intensity. *Limnology and Oceanography*, 1(2): 61-70.
- Ryther, J.H., 1969. Photosynthesis and Fish Production in the Sea. *Science*, 166: 72-76.

- Sakshaug, E., Demers, S. and Yentsch, C.M., 1987. *Thalassiosira oceanica* and *T. pseudonana*: two different photoadaptational responses. Marine Ecology Progress Series, 41: 275-282.
- Sakshaug, E., Johnsen, G., Andresen, K. and Vernet, M., 1991. Modeling of light-dependent algal photosynthesis and growth: experiments with the Barents Sea diatoms *Thalassiosira nordenskioeldii* and *Chaetoceros furcellatus*. Deep-Sea Research, 38(4): 415-430.
- Siegel, D.A., Michaels, A.F., Sorensen, J.C., O'Brien, M.C. and Hammer, M.A., 1995. Seasonal variability of light availability and utilization in the Sargasso Sea. Journal of Geophysical Research, 100(C5): 8695-8713.
- Smayda, T.J., 1980. Phytoplankton species succession. In: I. Morris (Editor), The Physiological ecology of phytoplankton. Studies in ecology. University of California Press, Berkeley, pp. 493-570.
- Strickland, J.D.H. and Parsons, T.R., 1972. A practical handbook of sea water analysis. Bulletin Fisheries Research Board of Canada, 167, Ottawa, 311 pp.
- Strom, S.L., Miller, C.B. and Frost, B.W., 2000. What sets lower limits to phytoplankton stocks in high-nitrate, low-chlorophyll regions of the open ocean? Marine Ecology-Progress Series, 193: 19-31.
- Sullivan, C.W., 1976. Diatom mineralization of silicic acid. I. $\text{Si}(\text{OH})_4$ transport characteristic in *Navicula pelliculosa*. Journal of Phycology, 12: 390-396.
- Sullivan, C.W., 1977. Diatom mineralization of silicic acid. II Regulation of $\text{Si}(\text{OH})_4$ transport rates during the cell cycle of *Navicula pelliculosa*. Journal of Phycology, 13: 86-91.
- Takeda, S., 1998. Influence of iron availability on nutrient consumption ratio of diatoms in oceanic waters. Nature, 393: 774-777.
- Thompson, P., 1999. The response of growth and biochemical composition to variations in daylength, temperature, and irradiance in the marine diatom *Thalassiosira pseudonana* (Bacillariophyceae). Journal of Phycology, 35: 1215-1223.
- Tilman, D., 1977. Resource Competition between Plankton Algae: An Experimental and Theoretical Approach. Ecology, 58: 338-348.
- Tyrrell, T., 2000. *Emiliana huxleyi* Statistics.
- Tyrrell, T. and Taylor, A.H., 1995. A modelling study of *Emiliana huxleyi* in the NE Atlantic. Journal of Marine Systems, 9(1-2): 83-112.
- Arrigo, K.R. and Sullivan, C.W., 1992. The influence of salinity and temperature covariation on the photophysiological characteristic of antarctica sea ice microalgae. Journal of Phycology, 28: 746-756.
- Balch, W.M., Kilpatrick, K.A., Holligan, P., Harbour, D. and Fernandez, E., 1996a. The 1991 coccolithophore bloom in the central North Atlantic .2. Relating optics to coccolith concentration. Limnology and Oceanography, 41(8): 1684-1696.
- Balch, W.M., Kilpatrick, K.A. and Trees, C.C., 1996b. The 1991 coccolithophore bloom in the central North Atlantic .1. Optical properties and factors affecting their distribution. Limnology and Oceanography, 41(8): 1669-1683.
- Banse, K., 1995. Community Response to Ironex. Nature, 375(6527): 112-112.
- Bienfang, P.K., 1985. Size structure and sinking rates of various microparticulate constituents in oligotrophic Hawaiian waters. Mar. Ecol. Prog. Ser., 23(2): 143-151.

- Bienfang, P.K., Harrison, P.J. and Quarmby, L.M., 1982. Sinking rate response to depletion of nitrate, phosphate and silicate in four marine diatoms. *Mar. Biol.*, 67(3): 295-302.
- Bishop, J.K.B., 1989. Regional Extremes in Particulate Matter Composition and Flux: Effects on the Chemistry of the Ocean Interior. In: W.H. Berger, V.S. Smetacek and G. Wefer (Editors), *Productivity of the Ocean: Present and Past*. Life Science Research Report. Wiley, Chichester, pp. 117-137.
- Brand, L.E., 1982. Genetic variability and spatial patterns of genetic differentiation in the reproductive rates of the marine coccolithophores *Emiliania huxleyi* and *Gephyrocapsa oceanica*. *Limnology and Oceanography*, 27(2): 236-245.
- Brand, L.E., 1994. Physiological ecology of marine coccolithophores.
- Brand, L.E. and Guillard, R.R.L., 1981. The Effects of Continuous Light and Light Intensity on the Reproduction Rates of Twenty-Two Species of Marine Phytoplankton. *J. Exp. Mar. Biol. Ecol.*, 50: 2-3.
- Brzezinski, M.A., 1985. The Si:C:N ratio of marine diatoms: Interspecific variability and the effect of some environmental variables. *J. Phycol.*, 21(3): 347-357.
- Busby, W.F. and Lewin, J., 1967. Silicate uptake and Silica shell formation by synchronously dividing cell of the diatom *Navicula pelliculosa* (Bréb.) Hilse. *Journal of Phycology*, 3: 127-131.
- Chisholm, S.W., Morel, F.M.M. and Slocum, W.S., 1980. The phasing and distribution of cell division. In: P.G. Falkowski (Editor), *Primary Productivity in the Sea*. Environmental Science Research. Plenum Press, NY, pp. 281-300.
- Cloern, J.E., 1977. Effect of light intensity and temperature on *Cryptomonas ovata* (Crptophyceae) growth and nutrient uptake rates. *Journal of Phycology*, 13: 389-395.
- Connell, J.H., 1978. Diversity in Tropical Rain Forests and Coral Reefs. *Science*, 199: 1302-1310.
- Daly, K.L. and Smith, W.O.J., 1993. Physical-Biological Interactions Influencing Marine Plankton Production. *Annual Review of Ecology and Systematics*, 24: 555-585.
- Davidson, K. and Gurney, W.S.C., 1999. An investigation of non-steady-state algal growth. II. Mathematical modelling of co-nutrient-limited algal growth. *Journal of Plankton Research*, 21(5): 839-858.
- Davidson, K., Wood, G., John, E.H. and Flynn, K.J., 1999. An investigation of non-steady-state algal growth. I. An experimental model ecosystem. *Journal of Plankton Research*, 21(5): 811-837.
- Droop, M.R., 1973. Some thoughts on nutrient limitation in algae. *Journal of Phycology*, 9: 264-272.
- Dugdale, R.C. and Wilkerson, F.P., 1998. Silicate regulation of new production in the equatorial Pacific upwelling. *Nature*, 391: 270-273.
- Egge, J.K. and Aksnes, D.L., 1992. Silicate as regulating nutrient in phytoplankton competition. *Mar. Ecol. Prog. Ser.*, 83: 281-289.
- Eppley, R.W., 1972. Temperature and phytoplankton growth in the sea. *Fisheries Bulletin*, 70: 1063-1085.
- Eppley, R.W., Rogers, J.N., McCarhy, J.J. and Sournia, A., 1971. Light/Dark periodicity in nitrogen assimilation of the marine phytoplankters *Skeletonema costatum* and

- Coccolithus huxleyi* in N-limited chemostat culture. *Journal of Phycology*, 7: 150-154.
- Eppley, R.W., Rogers, J.N. and McCarthy, J.J., 1969. Half-Saturation constant for uptake of nitrate and ammonium by marine phytoplankton. *Limnology and Oceanography*, 14: 912-920.
- Falkowski, P.G., Barber, R.T. and Smetacek, V., 1998. Biogeochemical Controls and Feedbacks on Ocean Primary Production. *Science*, 281: 200-206.
- Falkowski, P.G. and Raven, J.A., 1997. *Aquatic photosynthesis*, 375 pp.
- Fisher, T.R. and Butt, A.J., 1994. The Role of Nitrogen and Phosphorus in Chesapeake Bay Anoxia. In: S. Nelson and P. Elliot (Editors), *Perspectives on Chesapeake Bay, 1994. Advances in Estuarine Sciences*. Chesapeake Bay Program's Scientific and Technical Advisory Committee (STAC).
- Goldman, J.C. and Ryther, J.H., 1976. Temperature species competition in mass cultures of marine influenced phytoplankton. *Biotechnol. Bioengng*, 18: 1125-44.
- Grasshoff, K., 1976. *Methods of seawater analysis*, New York, 317 pp.
- Grover, J.P., 1988. Dynamics of Competition in a Variable Environment: Experiments with Two Diatom Species. *Ecology*, 69(2): 408-417.
- Grover, J.P., 1989. Phosphorus-dependent growth kinetics of 11 species of freshwater algae. *Limnol. Oceanogr.*, 34(2): 341-348.
- Grover, J.P., 1991. Resource competition environment: phytoplankton growing according to the variable-internal-stores model. *The American Naturalist*, 138(4): 811-835.
- Guillard, R.R.L., 1975. Culture of phytoplankton for feeding marine invertebrates. In: W.L.S.a.M.H. Chanley (Editor), *Culture of Marine Invertebrate Animals*. Plenum Press, New York, pp. 26-60.
- Guillard, R.R.L. and Ryther, J.H., 1962. Studies of marine planktonic diatoms. I. *Cyclotella nana* Hustedt and *Detonula confervacea* Cleve. *Can. J. Microbiol*, 8: 229-239.
- Hedges, J.I., 1992. Global biogeochemical cycles: progress and problems. *Marine Chemistry*, 39: 67-93.
- Hein, M. and Riemann, B., 1995. Nutrient Limitation of Phytoplankton Biomass or Growth-Rate - an Experimental Approach Using Marine Enclosures. *Journal of Experimental Marine Biology and Ecology*, 188(2): 167-180.
- Hulburt, E.M., 1970. Competition for nutrients by marine phytoplankton in oceanic, coastal, and estuarine reions. *Ecology*, 51(3): 475-484.
- Kirk, J.T.O., 1983. *Light and Photosynthesis in Aquatic Ecosystem*. Cambridge Univ. Press, Cambridge, 401 pp.
- Kolber, Z., Prasil, O. and Falkowski, P.G., 1998. Measurements of variable chlorophyll fluorescence using fast repetition rate techniques: defining methodology and experimental protocols. *Biochimica et Biophysica Acta*, 1367: 88-106.
- Lewis, M.R., Horne, E.P.W., Cullen, J.J., Oakey, N.S. and Platt, T., 1984. Turbulent mixing may control photosynthesis in the upper ocean. *Nature*, 311(5981): 49-50.
- Li, W.K.W., 1985. Photosynthetic response to temperature of marine phytoplankton along a latitudinal gradient (16°N to 74°N). *Deep-Sea Research*, 32(11): 1381-1391.
- Litchman, E. and Klausmeier, C.A., 2001. Competition of phytoplankton under fluctuating light. *American Naturalist*, 157(2): 170-187.

- Longhurst, A.R. and Harrison, W.C., 1989. The biological pump: profiles of plankton production and consumption in the upper ocean. *Progress in Oceanography*, 22: 47-123.
- Margalef, R., 1960. Temporal succession and spatial heterogeneity in phytoplankton. In: A.A. Buzzati-Traverso (Editor), *Perspectives in marine biology*. University of California Press, Berkeley, pp. 323-349.
- Margalef, R., 1997. *Our Biosphere. Excellence in ecology*, 10. Ecology Institute, Oldendorf, 176 pp.
- Martin, J.H., 1992. Iron as a limiting factor in Primary Productivity and Biogeochemical Cycles in the Sea. In: P.G. Falkowski, Woodhead, A. (Editor). *Plenum Press*, New York, NY, pp. 123-137.
- Mitchell, B.G., Brody, E.A., Holm-Hansen, O., McClain, C. and Bishop, J., 1991. Light limitation of phytoplankton biomass and macronutrient utilization in the Southern Ocean. *Limnology and Oceanography*, 36(8): 1662-1677.
- Monod, J., 1950. La technique de la culture continue: theorie et applications. *Ann. Ist. Pasteur Lille*: 390-410.
- Morel, A., 1978. Available, usable, and stored energy in relation to marine photosynthesis. *Deep-Sea Research*, 25: 673-688.
- Morin, P.J., 1999. *Community Ecology*. Blackwell Science, Malden, 424 pp.
- Muggli, D.L. and Harrison, P.J., 1996. Effects of nitrogen source on the physiology and metal nutrition of *Emiliania huxleyi* grown under different iron and light conditions. *Marine Ecology Progress Series*, 130: 255-267.
- Muggli, D.L. and Harrison, P.J., 1997. Effects of iron on two oceanic phytoplankton grown in natural NE subArctic Pacific seawater with no artificial chelators present. *Journal of Experimental Marine Biology and Ecology*, 212(2): 225-237.
- Nelson, D.M. and Brand, L.E., 1979. Cell division periodicity in 13 species of marine phytoplankton on a light:dark cycle. *Journal of Phycology*, 15: 65-75.
- Olsen, S. and Paasche, E., 1986. Variable Kinetics of Silicon -limited Growth in *Thalassiosira pseudonana* (Bacillariophyceae) in Response to Changed Chemical Composition of the Growth Medium. *British phycology Journal*, 21(183-190).
- Paasche, E., 1967. Marine Plankton Algae Grown with Light-Dark Cycles, I. *Coccolithus huxleyi*. *Physiologia Plantarum*, 20: 946-956.
- Paasche, E., 1973. Silicon and the Ecology of Marine Plankton Diatoms. I. *Thalassiosira pseudonana* (Cyclotella nana) Grown in a Chemostat with Silicate as Limiting Nutrient. *Marine Biology*, 19: 117-126.
- Paasche, E., 1980. Silicon content of five marine plankton diatom species measured with a rapid filter method. *Limnol. Oceanogr.*, 25(3): 474-480.
- Payne, C.D. and Price, N.M., 1999. Effects of cadmium toxicity on growth and elemental composition of marine phytoplankton. *Journal of Phycology*, 35(2): 293-302.
- Peterson, D.H., Perry, M.J., Bencala, K.E. and Talbot, M.C., 1987. Phytoplankton Productivity in Relation to Light Intensity: A Simple Equation. *Estuarine, Coastal and Shelf Science*, 24: 813-832.
- Platt, T. and Jassby, A.D., 1976. The relationship between photosynthesis and light for natural assemblages of coastal marine phytoplankton. *Journal of Phycology*, 12: 421-430.

- Raven, J.A., 1997. The vacuole: A cost-benefit analysis. *Advances in Botanical Research Incorporating Advances in Plant Pathology*, Vol 25, 25: 59-86.
- Riegman, R., Stolte, W., Noordeloos, A.A.M. and Slezak, D., 2000. Nutrient uptake and alkaline phosphatase (EC 3:1:3:1) activity of *Emiliana huxleyi* (Prymnesiophyceae) during growth under N and P limitation in continuous cultures. *J. Phycol.*, 36(1): 87-96.
- Ryther, J.H., 1956. Photosynthesis in the Ocean as a Function of Light Intensity. *Limnology and Oceanography*, 1(2): 61-70.
- Sakshaug, E., Demers, S. and Yentsch, C.M., 1987. *Thalassiosira oceanica* and *T. pseudonana*: two different photoadaptational responses. *Marine Ecology Progress Series*, 41: 275-282.
- Smayda, T.J., 1980. Phytoplankton species succession. In: I. Morris (Editor), *The Physiological ecology of phytoplankton. Studies in ecology*. University of California Press, Berkeley, pp. 493-570.
- Strickland, J.D.H. and Parsons, T.R., 1972. A practical handbook of sea water analysis. *Bulletin Fisheries Research Board of Canada*, 167, Ottawa, 311 pp.
- Sullivan, C.W., 1976. Diatom mineralization of silicic acid. I. Si(OH)_4 transport characteristic in *Navicula pelliculosa*. *Journal of Phycology*, 12: 390-396.
- Sullivan, C.W., 1977. Diatom mineralization of silicic acid. II Regulation of Si(OH)_4 transport rates during the cell cycle of *Navicula pelliculosa*. *Journal of Phycology*, 13: 86-91.
- Tilman, D., 1977. Resource Competition between Plankton Algae: An Experimental and Theoretical Approach. *Ecology*, 58: 338-348.
- Tyrrell, T., 2000. *Emiliana huxleyi* Statistics.
- Tyrrell, T. and Taylor, A.H., 1995. A modelling study of *Emiliana huxleyi* in the NE Atlantic. *Journal of Marine Systems*, 9(1-2): 83-112.
- Walsh, J.J., 1971. Relative Importance of Habitat Variables in Predicting the Distribution of Phytoplankton at the Ecotone of the Antarctic Upwelling Ecosystem. *Ecological Monographs*, 41(4): 291-309.
- Watabe, N. and Wilburn, K.M., 1966. Effects of temperature on growth, calcification, and coccolith form in *Coccolithus huxleyi* (Coccolithineae). *Limnology and Oceanography*, 11(4): 567-575.
- Walsh, J.J., 1971. Relative Importance of Habitat Variables in Predicting the Distribution of Phytoplankton at the Ecotone of the Antarctic Upwelling Ecosystem. *Ecological Monographs*, 41(4): 291-309.
- Watabe, N. and Wilburn, K.M., 1966. Effects of temperature on growth, calcification, and coccolith form in *Coccolithus huxleyi* (Coccolithineae). *Limnology and Oceanography*, 11(4): 567-575.
- Watson, A.J., Bakker, D.C.E., Ridgwell, A.J., Boyd, P.W. and Law, C.S., 2000. Effect of iron supply on Southern Ocean CO_2 uptake and implications for glacial atmospheric CO_2 . *Nature*, 407(6805): 730-733.
- Werner, D., 1977. *The Biology of Diatoms. Botanical Monographs*, 13. Univ. of California Press., 498 pp.
- Wyman, M., Daviesa, J.T., Westonb, K., Crawford, D.W. and Purdie, D.A., 1998. Ribulose-1,5-bisphosphate Carboxylase/oxygenase (RubisCO) Gene Expression and

Photosynthetic Activity in Nutrient-enriched Mesocosm Experiments. *Estuarine, Coastal and Shelf Science*, 46(2): 23-33.

Acknowledgments

I would like to sincerely thank those that made the results presented in this thesis possible and in helping me reach another step in my academic career. First, I would like to thank my advisor Paul Falkowski for providing me the incredible opportunity to work in his group at the Institute of Marine and Coastal Sciences of Rutgers University. This experience exposed me to an exorbitant amount of knowledge, practice and to many kindhearted people. I would also like to thank the other members of my committee, Oscar Schofield and Peter Morin. Oscar was patient and generous, always ready to discuss any issue with me as a teacher and as a friend. I thank Peter for valuable guidance helping me approach my ecology questions in a scientifically valid way. I need to also thank Kevin Wyman for technical assistance, algae culturing, CHN analysis and general lab needs. A thanks goes to Renée Styles, Ron Lauck and Tracy Wiegner for training me in the use of the Autoanalyzer, and to Jessie Sebbo for support in some of the experimental work. I thank Andrew Irwin for the help and support in developing the codes for the numerical models, Antonietta Quigg, Zoe Finkel and Joe Grzyski for valuable discussions and critical reading of the thesis. Emmeline Romana was integral in with administrative and logistic problems. I would also like to thank Debora Iglesias, Jay Cullen and my officemate Trisha Bergmann for being good and encouraging friends from the beginning of my experience at the institute and in the United States. Finally I would like to thank my family back in Italy and my former advisor Maurizio Ribera d'Alcala' for introducing me to oceanography, teaching me the importance of an interdisciplinary approach to science and how to enjoy and love my work.

NASA – SMP “Representing Key Phytoplankton Groups in Ocean Carbon Cycle Models” Grant: NAG5-6982. Rutgers University also gave me the wonderful opportunity, supporting my research for a semester to TA Oceanographic Methods and Data Analysis (11:628:364).